Coral Reefs
https://doi.org/10.1007/s00338-021-02138-2

REPORT

Chronic low-level nutrient enrichment benefits coral thermal performance in a fore reef habitat

Danielle M. Becker[1,2] · Hollie M. Putnam[2] · Deron E. Burkepile[3,4] · Thomas C. Adam[3] · Rebecca Vega Thurber[5] · Nyssa J. Silbiger[1]

Received: 31 August 2020 / Accepted: 14 June 2021

Abstract Global- and local-scale anthropogenic stressors have been the main drivers of coral reef decline, causing shifts in coral reef community composition and ecosystem functioning. Excess nutrient enrichment can make corals more vulnerable to ocean warming by suppressing calcification and reducing photosynthetic performance. However, in some environments, corals can exhibit higher growth rates and thermal performance in response to nutrient enrichment. In this study, we measured how chronic nutrient enrichment at low concentrations affected coral physiology, including endosymbiont and coral host response variables, and holobiont metabolic responses of *Pocillopora* spp. colonies in Mo'orea, French Polynesia. We experimentally enriched corals with dissolved inorganic nitrogen and phosphate for 15 months on an oligotrophic fore reef in Mo'orea. We first characterized symbiont and coral physiological traits due to enrichment and then used thermal performance curves to quantify the relationship between metabolic rates and temperature for experimentally enriched and control coral colonies. We found that endosymbiont densities and total tissue biomass were 54% and 22% higher in nutrient-enriched corals, respectively, relative to controls. Algal endosymbiont nitrogen content cell^{-1} was 44% lower in enriched corals relative to the control colonies. In addition, thermal performance metrics indicated that the maximal rate of performance for gross photosynthesis was 29% higher and the rate of oxygen evolution at a reference temperature (26.8 °C) for gross photosynthesis was 33% higher in enriched colonies compared to the control colonies. These differences were not attributed to symbiont community composition between corals in different treatments, as C42, a symbiont type in the *Cladocopium* genus, was the dominant endosymbiont type found in all corals. Together, our results show that in an oligotrophic fore reef environment, nutrient enrichment can cause changes in coral endosymbiont physiology that increase the performance of the coral holobiont.

Topic Editor Simon Davy

✉ Danielle M. Becker
danielle.becker.927@my.csun.edu

Hollie M. Putnam
hputnam@uri.edu

Deron E. Burkepile
deron.burkepile@lifesci.ucsb.edu

Thomas C. Adam
thomas.adam@lifesci.ucsb.edu

Rebecca Vega Thurber
rvegathurber@gmail.com

Nyssa J. Silbiger
nyssa.silbiger@csun.edu

[1] Department of Biology, California State University, Northridge, CA 91330, USA

[2] Department of Biological Sciences, University of Rhode Island, 120 Flagg Rd, Kingston, RI 02881, USA

[3] Marine Science Institute, University of California, Santa Barbara, CA 93106, USA

[4] Department of Ecology, Evolution and Marine Biology, University of California, Santa Barbara, CA 93106, USA

[5] Department of Microbiology, Oregon State University, Corvallis, OR 97333, USA

Published online: 29 June 2021

Keywords Nutrient enrichment · *Pocillopora* spp. · Thermal performance curve · Coral physiology · Fore reef

Introduction

Coral reef ecosystems facilitate complex ecological relationships and provide critical economic services around the world (Wilkinson 2008; Cisneros-Montemayor and Sumaila 2010; Brander et al. 2015). The symbiosis between reef-building corals and their diverse algal endosymbionts, members of the family Symbiodiniaceae (LaJeunesse et al. 2018), provide carbon to corals in excess of the host respiratory energy requirements through translocation of products from photosynthetic carbon fixation (Muscatine et al. 1984), allowing corals to thrive in nutrient-poor tropical waters (Kinzie et al. 2018). This vital symbiosis can be decoupled by coral bleaching, when corals expel or lose their endosymbionts, a phenomenon that is caused by changes in environmental conditions; primarily, thermal anomalies associated with rising sea surface temperatures (Hughes et al. 2018). Mass coral bleaching events have been a main driver of coral reef decline over the last century and in some locations have resulted in shifts from coral-dominated to algal-dominated reef communities, leading to altered ecosystem functioning (Hughes et al. 2003; van de Leemput et al. 2017). Further, local-scale stressors that occur in nearshore reef environments, including eutrophication and sedimentation, can make corals more vulnerable to global climate change by suppressing calcification (Shantz and Burkepile 2014), driving changes in microbiome communities (Zaneveld et al. 2016; McDevitt-Irwin et al. 2017; Wang et al. 2018), and reducing their photosynthetic performance (Nordemar et al. 2003; Silverman et al. 2007). Because multiple stressors occur simultaneously in the ocean (Halpern et al. 2015), understanding how they interact can help predict how benthic reef communities may change in the future.

Local-scale stressors affect the biological and physiological responses of corals to thermal stress. Many studies have found that local-scale stressors (e.g., nutrient loading, sedimentation, and fishing pressures) can exacerbate the impacts of thermal stress on coral species (Dubinsky and Stambler 1996; Tanaka et al. 2014; Humanes et al. 2017; Serrano et al. 2018). For example, when nutrient enrichment is coupled with elevated seawater temperature, *Porites cylindrica* primary production rate and tissue biomass decreases (Nordemar et al. 2003). In larval *Diploria strigosa*, development is slowed or halted (Bassim and Sammarco 2003), settlement rates are reduced (Bassim and Sammarco 2003), and larval mortality increases (Serrano et al. 2018) when exposed to both nutrient enrichment and elevated seawater temperature. Further, nutrient enrichment can impair the complex coral–algal symbioses and facilitate bleaching in coral colonies (Cunning and Baker 2013; Wiedenmann et al. 2013; Wooldridge 2013; Vega Thurber et al. 2014; Burkepile et al. 2020). Yet, in other cases, nutrients have been shown to be beneficial to corals by increasing their growth rates (Koop et al. 2001; Bongiorni et al. 2003; Dunn et al. 2012) and reducing corals susceptibility to bleaching (McClanahan et al. 2003). Further, coral reef habitats that experience natural processes like upwelling and internal waves, which bring cool, nutrient-rich water from deeper depths, have been suggested as possible refuges for corals (Szmant and Forrester 1996; Riegl and Piller 2003). The impacts of nutrient enrichment, especially dissolved inorganic nutrients, on the physiological responses of corals to elevated temperature are still actively debated (Morris et al. 2019; Fernandes et al. 2020) because the relationships between nutrients, temperature, and coral physiology can vary depending on geographic region, oceanographic condition, and/or reef environment (Szmant 2002; D'Angelo and Wiedenmann 2014; Shantz and Burkepile 2014).

Many confounding variables like light, sedimentation, and temperature influence how corals respond to thermal stress under eutrophic conditions (Rogers 1990; Dubinsky and Stambler 1996; Fabricius 2005), making it difficult to uncover specific mechanisms in studies using natural gradients that lead to variation in coral metabolic processes (i.e., photosynthesis, respiration, and calcification). Fore reef habitats experience mostly natural forms of nutrient inputs, including recycled nutrient products from fish excretions and nitrogen fixation by diazotrophs (e.g., cyanobacteria) (Kayanne et al. 2005; O'Neil and Capone 2008; Charpy et al. 2012; Shantz and Burkepile 2014; Allgeier et al. 2016). Upwelling events and internal waves bring nutrient-rich water to the oligotrophic surface ocean waters (D'Croz et al. 2001; Schlöder and D'Croz 2004; Radice et al. 2019). Naturally occurring forms of nutrient enrichment have been shown to elevate coral reef productivity (Wolanski and Delesalle 1995a) and enhance scleractinian coral growth, in terms of calcification rates, skeletal densities, and linear extension (Shantz and Burkepile 2014). Further, when exposed to upwelling, coral species have been shown to readily acclimate to increasing temperatures (Mayfield et al. 2013), increase coral growth rates (Leichter and Genovese 2006), and exhibit resilience to ocean acidification (Griffiths et al. 2019). Therefore, manipulating nutrient concentrations in environments further from the coastline with less covarying factors than typically found in a fringing reef habitat can help us understand how nutrients specifically affect the physiological responses of corals under thermal stress.

In this study, we deployed a 15-month nutrient enrichment experiment to test the influence of in situ nutrient loading on *Pocillopora* spp. thermal performance on the fore reef in Mo'orea, French Polynesia. While there are numerous studies investigating how nutrient fluxes affect coral physiology (Fabricius 2005; Ezzat et al. 2016; Kitchen et al. 2020), there is limited information on the effects of low nutrient exposure on the thermal performance of corals (Wiedenmann et al. 2013; D'Angelo and Wiedenmann 2014). The goal of this study was to investigate how in situ, chronic, low-level nutrient enrichment influences (1) the ability for endosymbiont and coral host response variables to contribute to the metabolic functionality of the holobiont and (2) how coral thermal performance metrics shift in response to different nutrient regimes. Here, we use a thermal performance curve approach (TPC; Sharpe and Demichele 1977; Schoolfield et al. 1981; Schulte et al. 2011) to quantify the shape of the relationship between the control and nutrient enrichment for TPC metrics of gross photosynthesis (GP) and dark respiration (R_d) rates as a function of increasing temperature (ramp from 20 to 38 °C). We extracted TPC metrics including (1) acute thermal optimum (T_{opt}), which is the temperature at which the organism is at its (2) maximal rate of performance (μ_{max}), and (3) the rate at a reference temperature (b(T_c)) which is often used to compare standardized rates of performance across populations (Angilletta Jr. 2009; Andrews and Schwarzkopf 2012), species (Dell et al., 2011; Sinclair et al., 2012; Bestion et al., 2018), or geographic regions (Angilletta Jr. 2009; Sgrò et al., 2010; Aichelman et al., 2019; Jurriaans and Hoogenboom, 2019; Silbiger et al., 2019). Based on prior research on the relationship between nutrient enrichment and the physiological response of corals to thermal stress (Ezzat et al. 2016; Morris et al. 2019; Kitchen et al. 2020; Krueger et al. 2020), we hypothesized that chronic low-level nutrient enrichment (i.e., nitrogen and phosphorus) will increase endosymbiont densities, chlorophyll *a* content, tissue biomass, and N content, shift endosymbiont community composition, and result in increased thermal performance of corals (D'Angelo and Wiedenmann 2014; Morris et al. 2019).

Materials and methods

Site description

Mo'orea, French Polynesia, is a volcanic island located in the central South Pacific ~ 20 km west of Tahiti. Mo'orea has an offshore barrier reef that surrounds the 60 km perimeter with systems of shallow (mean depth < 3 m) and narrow (~ 0.8–1.5 km wide) lagoons. The barrier reef is ~ 0.5–1.5 km from the shore, and the inshore lagoons are protected, but connected to the open ocean, through a series of passes. The fore reef habitats are composed of coral spur-and-groove formations that run perpendicular to the reef crest from 2 to > 60 m in depth (Leichter et al. 2013). The fore reef habitats experience high water movement associated with strong wave action from incoming waves that break on the reef crest causing a gradual swell and wave attenuation toward deeper depths (Wolanski and Delesalle 1995a, 1995b; Monismith 2007; Leichter et al. 2013; Dubé et al. 2017).

Two fore reef sites on the north shore of Mo'orea, French Polynesia, were chosen for a nutrient-enriched treatment and a control. The treatment sites were ~ 20 m apart to reduce any confounding variables. Four sample blocks were established at each site, ~ 5 m apart from each other. Five nutrient diffusers were placed in each block on a north shore fore reef site in July 2018, representing the nutrient-enriched site (S17° 28.386′ W149° 49.059′) (Fig. 1a, b, c). The control site was devoid of nutrient diffusers (S17° 28.38′ W149° 49.03′) (Fig. 1a, b, d). Osmocote® pellets were placed in a diffuser (diffusion tube), which consisted of a 15 cm long × 2.5 cm wide PVC pipe with 10, 1-cm holes drilled into the side and covered in a mesh screen. Each nutrient diffuser consisted of 175 g Osmocote ® (The Scotts Company, Marysville, Ohio, USA) slow release garden fertilizers (19:6:12, N:P:K), containing nitrite (NO_2^-), nitrate (NO_3^-), ammonium (NH_4^+), phosphate (PO_4^{3-}), and potassium (K), with no trace metals. Osmocote® diffusers are an efficient method of enriching water column nutrients near the benthos (Worm and Sommer 2000; Burkepile and Hay 2009). The nutrient diffusers were secured to the benthos with cable ties attached to stainless steel all-thread posts that were drilled into the reef framework (Fig. 1c). Nutrient diffusers were exchanged every 12–16 weeks to ensure continuous delivery of nutrients to the experiment based on previously tested nutrient depletion rates (Burkepile et al. 2020). The nutrient diffusers were last exchanged on August 30, 2019, roughly two months prior to our collection and experimental period.

Quantifying nutrient regimes between enriched and control treatments

Percent tissue nitrogen (N) of *Lobophora variegata* was calculated from duplicate *L. variegata* individuals per sample block at each site (n = 8 per treatment) at the same time the corals were collected for fragmentation. Macroalgal % N content is a more useful long-term integrated measure of seawater nutrient loading (Fong et al. 1994; Lin and Fong 2008) compared to water column nutrient samples as it can inform us on what the benthos

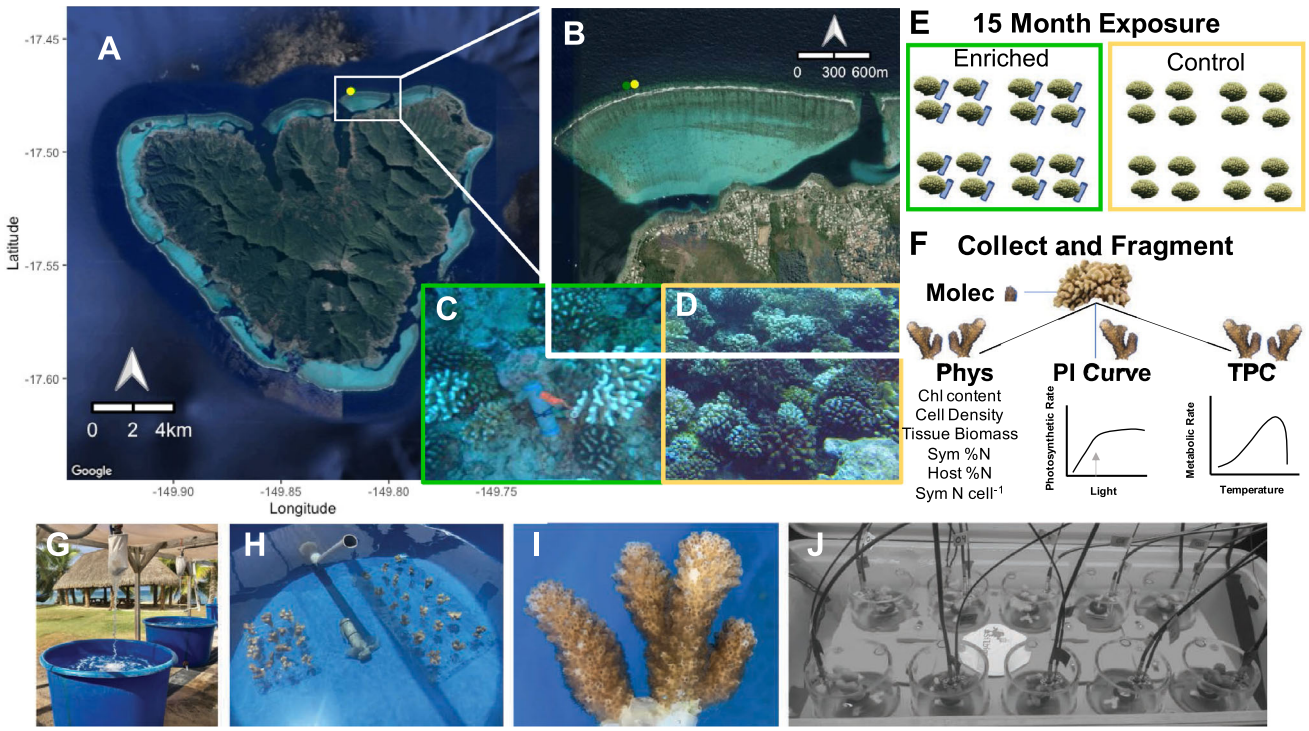

Fig. 1 **a** Map of Mo'orea, French Polynesia identifying **b** the study sites for *Pocillopora* spp. sampling along the north shore fore reefs. The green bordered photograph shows **c** a nutrient diffuser at a nutrient-enriched site and the yellow bordered photograph **d** shows an example of a control site on the fore reef. The experimental design included a **e** 15-month exposure to the enriched or control conditions (n = 16 colonies per treatment), followed by collection of **f** molecular samples (n = 16 nubbins per treatment), characterization of physiological state (n = 32 nubbins per treatment), and identification of saturating irradiance using PI curves (indicated by the gray arrow, n = 4 nubbins per treatment). Two fragments per colony were placed into continued exposure tanks **g–i**) until they were exposed to a thermal ramp of 10 temperatures (20–38 °C) in a (J) 10 chamber setup

experiences over weeks or months compared to an instantaneous water column sample. Approximately 1 g (wet mass) of tissue was removed from each individual, rinsed in freshwater (FW) where epiphytes were removed manually with forceps, and dried to constant weight at 80 °C (Carpenter 2018). Dried samples were submitted for CHN analysis by the means of high-temperature (1000 °C) combustion following Dumas method (Shea and Watts 1939) of samples in an oxygen-enriched helium atmosphere in an elemental analyzer (Control Equipment Corporation: Model CEC 440HA, North Chelmsford, MA, USA) at the University of California, Santa Barbara Marine Science Institutes (UCSB MSI) Analytical Lab.

One water column sample was collected < 0.5 m away from the nutrient diffusers at each sampling block (n = 4 samples per treatment) to characterize nutrient concentrations in the seawater at the time of coral collection. Water column samples were collected from above the benthos using 60-mL lip-lock tip syringes for dissolved inorganic NO_3^- + NO_2^-, NH_4^+, and PO_4^{3-}. The samples were filtered through a 0.7 µm GF/F (Whatman ®, Maidstone, UK) and the seawater samples were placed in a −20 °C freezer immediately upon returning to the University of California, Berkeley Richard B. Gump South Pacific Research Station (UCB Gump Station). Dissolved inorganic nutrients (PO_4^{3-}, NO_3^- + NO_2^-, NH_4^+) were analyzed using flow injection (QuikChem 8500 Series 2, Lachat Instruments, Zellweger Analytics, Inc., Loveland, CO, USA) at the UCSB MSI Analytical Lab (Johnson et al. 1985). Dissolved inorganic nitrogen-to-phosphorus (DIN:DIP) ratios were calculated by the summation of [NO_3^- + NO_2^- + NH_4^+] for DIN and [PO_4^{3-}] for DIP. The DIN:DIP ratios are expressed on a molar basis.

Coral collection

Our study was conducted following 15 months of nutrient enrichment (Fig. 1e) during October 2019 at the control and nutrient-enriched sites on the north shore fore reef habitat in Mo'orea (Fig. 1a–d). We collected fragments of *Pocillopora meandrina* at each site based on morphological characteristics (Maté et al. 2016). However, due to recent analyses on the complexity of *Pocillopora* spp. identification (Johnston et al. 2018; Burgess et al. 2021), morphological characteristics are unreliable for species identification. Therefore, the coral fragments will be

referred to as *Pocillopora* spp. for the remainder of the manuscript. Thirty-two *Pocillopora* spp. colonies showing no signs of bleaching were haphazardly collected in a block design with four fragments collected from each of four treatment or control blocks from depths of ~ 13 m. The treatment coral fragments were collected within < 0.5 m the nutrient diffusers for the nutrient-enriched treatment (n = 16) and ~ 20 m away from the diffusers for the control (n = 16) on October 15, 2019. *Pocillopora* spp. fragments were removed with hammer and chisel via SCUBA, placed in clean ziplock bags full of seawater, and returned to the boat.

To quantify the endosymbiont communities between our nutrient-enriched treatment and control sites, a small coral biopsy was collected from each coral fragment (n = 16 colony biopsies per treatment) (Fig. 1f). Biopsies were performed immediately after arrival at the boat by breaking a fragment ≤ 0.5 cm in any single dimension using the top of a sterile DNase, RNase, endotoxin-free 2.0-mL microcentrifuge tube with an O-ring cap (VWR ®, Cat # 16,466–044, Radnor, PA, USA), into which each biopsy was placed with 1.0 mL of DNA/RNA Shield™ (Zymo Research, Cat #R1100-250, Irvine, CA, USA). Gloves were sterilized between each sample with a 10% bleach solution and freshwater rinse. The tissue samples were immediately placed on ice in a cooler on the boat and then transferred directly to a −80 °C freezer upon arrival at the UCB Gump Station.

The coral fragments for physiological assays were transported to the UCB Gump Station in a seawater filled cooler and immediately placed in flow-through seawater tables. Using a stainless steel diagonal cutter, fragments of each sample colony were cut into five replicate dimensions (7.8 cm × 7.8 cm) of multi-branch fragments, which were measured with calipers (Fig. 1f). Two fragments were used for light and dark respirometry trials, and two fragments were used for endosymbiont and coral response variables, including chlorophyll *a* content, endosymbiont densities, endosymbiont % nitrogen (N) content, endosymbiont N cell^{-1}, tissue biomass, and coral tissue % N content (Fig. 1f). A fifth fragment was randomly selected from four colonies per treatment to be used to determine saturating light conditions (Fig. 1f).

The two fragments delegated for endosymbiont and coral response variables (one for % tissue N and one for the remaining parameters) were immediately frozen at −20 °C until processing. The two fragments designated for photosynthesis and respiration trials were affixed to pre-labeled acrylic coral plugs (Industry, CA, USA) using hot glue around the base of the coral skeleton while the fragment was submerged (Fig. 1i). After coral fragments were affixed, they were placed into one of two flow-through holding tanks (either control or nutrient-enriched) with filtered (pore size ~ 100 µm) seawater to recover from the fragmentation process for 7–12 days (Fig. 1h). The coral plugs were placed in individual holes on an acrylic sheet with an O-ring placed around the bottom of the plug for stabilization (Fig. 1h). The acrylic bases had 4 small 15-cm tall PVC pipes on the four corners of the base to keep the corals from being in contact with the bottom of the tank (Fig. 1h). Holding tank conditions were designed to mimic temperature and light regimes found at the collection sites (Fig. 1g,h) (Carpenter 2018, 2019; Leichter et al. 2019).

Holding tank conditions

Temperature

Temperature was recorded in both holding tanks with HOBO® loggers (Onset® HOBO® TidbiT® v2 Temp Data Logger UTBI-001, Bourne, MA, USA, accuracy ± 0.21 °C from 0 to 50 °C) every 15 min during the recovery period (7–12 days). The mean (± SE) seawater temperature in the holding tanks was 26.9 ± 0.04 °C, which is consistent with the mean seawater temperature (~ 26.9 °C) at the collection site during October (Leichter et al. 2019).

Light

A tan shade cloth (SunScreen Fabric, Easy Gardener) canopy was installed above the holding tanks to mimic light conditions on the fore reef (Comeau et al. 2013, 2014; Carpenter 2019). Photon flux density (PFD) was measured daily in the holding tanks at three time points (08:00, 12:00, 16:00) using an underwater cosine corrected sensor (MQ-510 Quantum Meter Apogee Instruments, spectral range of 389–692 nm ± 5 nm, Logan, UT, USA). The sensor was placed at five separate points within each of the holding tanks each time, and an average daytime PFD measurement was taken for each day. The mean (± SE) daytime PFD in the holding tanks was 302 ± 43 µmol photons m^{-2} s^{-1} in the nutrient-enriched tank and 306 ± 44 µmol photons m^{-2} s^{-1} control tank, which is consistent with the mean daytime light photon flux density ranges experienced at similar depths on the forereef during October (Comeau et al. 2013, 2014; Carpenter 2019).

Nutrients

A slow release 175 g Osmocote ® (19–6-12, N-P-K) garden fertilizer was placed in the nutrient-enriched recovery tank (Fig. 1h), and the ambient tank was unmanipulated. Triplicate water samples were collected for dissolved inorganic nutrients following the methods above on the sixth day of the recovery period. Dissolved inorganic

$NO_3^- + NO_2^-$, NH_4^+, and PO_4^{3-} tank conditions were consistent with the conditions at the collection site (Fig. S1 in supplement file 1).

Endosymbiont and coral response variables

Nucleic acid extraction and sequencing

Half of the mass of the biopsy and DNA/RNA shield volume (500 µl) was transferred to a 2-mL microcentrifuge tube containing sterile 2 mL of 0.5 mm glass bead (Fisher Scientific Catalog. No 15–340-152). Samples were homogenized using a Qiagen Tissue Lyser for 40 s at 20 Hz. The resulting supernatant transferred to a sterile RNase–DNase-free 1.5-mL microfuge tube and DNA and RNA was simultaneously extracted using the Zymo Quick-DNA/RNA Miniprep Plus Kit Protocol according to manufacturer's instructions. RNA was stored at −80 °C, and DNA was quantified with a Broad-range DNA kit on a ThermoFisher Qubit Fluorometer. DNA quality was checked using gel electrophoresis on a 1.5% agarose gel in tris-acetate–EDTA buffer after running for 45 min at 100v. To identify the Symbiodiniaceae in the coral samples, the Internal Transcribed Spacer 2 (ITS2) region of the symbionts was amplified for sequencing using a two-step library preparation protocol. First, a master mix was generated containing 2 µL of 10 µM of forward (5′-TCGTCGGCAGCGTCAGATGTGTATAAGAGACAG-[GAATTGCAGAACTCCGTG-3′]; IT Sintfor2 in brackets; Howells et al. 2020) and reverse (5′-GTCTCGTGGGCTCGGAGATGTGTATAAGAGACAG-[GGGATCCATATGCTTAAGTTCAGCGGGT-3′]; ITS2-reverse in brackets; Howells et al. 2020) primers with an overhanging adapter sequence (sequence prior to brackets), 50 µL of 2X Phusion HiFi Mastermix (Thermo Scientific F531s), and 46 µL of DNase/RNase-free water. To avoid PCR bias, each sample was amplified in triplicate on 96-well plates with 33 µL of master and 1 µL of equal concentration DNA sample (3.33 ng/µl). Both a negative (10 µL of ultra-pure water) and positive control (0.5 µL of each sample as a mix) were included. Samples were amplified using polymerase chain reaction (PCR) with the following profile: 3 min at 95 °C, followed by 35 cycles of 30 s at 95 °C, 30 s at 52 °C, and 30 s at 72 °C, finished by 2 min at 72 °C and held indefinitely at 4 °C. The triplicate PCR products were run on a 2% agarose gel to confirm the presence of a band at the expected length of ~ 300 bp and stored at −20 °C. Samples with the overhanging adapter sequence that were verified to be the desired size and free of primer dimer were delivered to the Rhode Island Genomics and Sequencing Center (RIGSC). The RIGSC performed the second round of PCR which included between 5 and 10 cycles of PCR to attach Nextera indices and adapters. This product was then cleaned with Ampure XP, visualized using agarose gel electrophoresis, quantified on a ThermoFisher Qubit Fluorometer for pooling and finally quantified using QPCR for loading on the Illumina MiSeq. Samples were sequenced as paired ends, with 300 cycles for each read pair.

Tissue removal

An Iwata Eclipse HP-BCS airbrush (Portland, OR, USA) filled with filtered seawater (0.2 µm) was used to remove coral tissue from the frozen coral skeleton. The resulting coral tissue slurries ($n = 32$ total) were individually homogenized for 15 s at 3,000 rpm with an electric hand-held homogenizer (BT Lab Systems Saint Louis, MO, USA). Aliquots were taken from the tissue homogenate for each endosymbiont (chlorophyll *a* content, endosymbiont densities, % N content (% dry weight), and N content $cell^{-1}$) and coral response variable (tissue biomass and % N content (% dry weight)) and frozen at −20 °C until further processing. Coral skeletons were dried at 60 °C for 4 h in a drying oven (Fisher Scientific Isotemp Oven, Waltham, MA, USA). After the skeletons were dry, the surface area was measured by dipping the skeletons in a 65 °C Minerva Paraffin Wax bath (Monroe, GA, USA) for 2 s, before removal and then rotating them quickly in the air (10 revolutions over 2 s). The coral skeletons were cooled at room temperature prior to being weighed (Stimson and Kinzie III 1991; Veal et al. 2010). Surface area was calculated against a standard curve of mass change of wax dipped dowels against geometrically calculated surface area, with an $R^2 > 0.9$ for the relationship.

Algal endosymbiont densities

Replicate cell counts ($n = 6$–8) were conducted for aliquoted (1 mL) coral tissue slurry samples, using an Improved Neubauer Haemocytometer (Marienfeld Superior, Lauda-Königshofen, Germany) to quantify algal endosymbiont densities. The endosymbiont cell densities were then normalized to coral surface area (cells cm^{-2}) (Stimson and Kinzie III 1991; Veal et al. 2010).

Chlorophyll a content

Duplicate 3 mL samples from the tissue slurries were centrifuged (3,450 rpm × 3 min) (Fisher Scientific accuSpin™ 3R, Waltham, MA, USA) to isolate the algal pellet. 100% acetone was added to the algal pellet and placed in a freezer at −20 °C for 36 h in the dark. The supernatant of the extracted samples was measured spectrophotometrically ($\lambda = 630$, 663, and 750 nm) (Shimadzu UV-2450, Kyoto, Kyoto Prefecture, Japan), and concentrations of chlorophyll *a* were calculated using equations specified for dinoflagellates from Jeffrey and Humphrey

(1975), after accounting for an acetone blank. The chlorophyll concentrations were then normalized to surface area (μg cm^{-2}) and to endosymbiont cells (pg $cell^{-1}$).

Tissue biomass

Triplicate 1 mL aliquots from each coral tissue slurry ($n = 32$) were pipetted into pre-burned aluminum pans (450 °C for 5 h) and then placed in a drying oven (Fisher Scientific Isotemp Oven, Waltham, MA, USA) at 60 °C for > 24 h until they reached a constant weight. Once the samples had reached a constant weight, they were placed in a muffle furnace (Fisher Scientific Isotemp Muffle Furnace, Waltham, MA, USA) at 450 °C for 4–6 h to determine ash-free dry weight. The total biomass of the aliquoted tissue slurry was the difference between the dried (60 °C) and burned (4–6 h at 450 °C) masses and the tissue biomass was expressed as mg cm^{-2}.

Coral and endosymbiont tissue nitrogen content

To calculate coral tissue and endosymbiont N content, the skeletal carbonates were first separated from the host tissue and endosymbionts using a 20 μm nylon net filter (Wildco®, Yulee, FL, USA) (Maier et al. 2010) and the remaining host tissue and endosymbiont cells were separated by centrifugation (3,450 rpm × 3 min.) (Fisher Scientific accuSpin™ 3R, Waltham, MA, USA) with 3–4 seawater rinses (Muscatine et al. 1989). To ensure separation efficiency between the coral tissue and endosymbionts, microscopic inspections were conducted on the supernatant and the endosymbiont pellets using a Leica Binocular Microscope (DM500, Feasterville, PA, USA) between each seawater rinse and centrifugation. If animal constituents, like nematocysts or spirocysts, were observed in the endosymbiont pellets, the sample was repeatedly resuspended and centrifuged until the final endosymbiont pellet had been properly washed and animal constituents were no longer observed. The same resuspension and centrifuge steps were taken if any endosymbiont cells were observed in the supernatant. Tissues were filtered onto weighed pre-combusted 25 mm GF/F filters (Whatman ®, Maidstone, UK) (450 °C, 4 h), dried overnight (80 °C), weighed, and placed in microcentrifuge tubes (Wall et al. 2018). Due to the vacuum filtration method, we note that host tissue samples may underestimate the total C and N content, since soluble material and particulate matter less than 0.7 μm would be lost in the process. CHN content for the coral host's tissue and algal endosymbionts were analyzed at the UCSB MSI Analytical Lab using the same methods described above. Algal endosymbiont % N content and coral % N content were calculated by normalizing the N (mg) to the weight of the tissue on the filter (mg) and multiplying by 100. The N per algal endosymbiont cell (pg N $cell^{-1}$) was also calculated.

Holobiont metabolic response variables

Estimating saturating light levels

To measure photosynthetic rates during our experimental temperature assays, we first estimated saturating light levels from net photosynthesis–photon flux density curves (commonly referred to as photosynthesis–irradiance curves) for the collected corals (n = 8 fragments, 4 fragments from each site: Fig. 1f). Fragments were placed in identical closed-system acrylic respiration chambers (10 chambers, 650 ml each; Fig. 1j) (Australian Institute of Marine Science, Townsville, Australia) with filtered (pore size ~ 100 μm) seawater and rotating stir bars (200 rpm), including replicate seawater-only chambers ($n = 2$) as blanks for controls during each trial (Silbiger et al. 2019). Temperature (°C) and oxygen concentrations (μmol L^{-1}) were measured using Presens Temperature (Pt1000, Regensburg, Germany) and Presens Oxygen Dipping Probes (DP-PSt7, Regensburg, Germany) (company two-point calibration with oxygen-free environment [nitrogen, sodium sulfite] and air-saturated environment), respectively, at a frequency of 1 Hz. Measurements were taken using a Presens Oxygen Meter (OXY-10 SMA (G2) Regensburg, Germany) system with temperature correction for each channel separately. Temperature was held constant at 26.8 °C (± 0.1 °C) with a thermostat system (Apex Controller, Neptune Systems, Morgan Hill, CA, USA). An LED light (Mars Aqua 300w LED Brand Epistar, Long-Gang District, ShenZhen, China) was positioned above the chambers, and sequential photon flux densities (0, 23, 64, 145, 207, 304, 529, 739, 927 μmol m^{-2} s^{-1}) were used to identify a net photosynthesis–photon flux density curve fit in order to calculate saturating light (I_k) of the corals. Light levels were measured by an underwater cosine corrected sensor (MQ-510 Quantum Meter Apogee Instruments, spectral range of 389–692 nm ± 5 nm, Logan, UT, USA).

Rates of oxygen evolution and consumption were determined using repeated local linear regressions with the package *LoLinR* (Olito et al. 2017) in R (R Core Team 2013), with rates corrected for chamber volume displacement by the corals, blank seawater control rates, and normalized to coral surface area using the paraffin wax dipping technique (Stimson and Kinzie III 1991; Veal et al. 2010). *LoLinR* was run with the parameters of L_{pc} for linearity metric (L_{pc} = the sum of the percentile ranks of the Z_{min} scores for each component metric) and alpha = 0.6 (minimum window size for fitting the local regressions, which is the proportion of the total observations in the data set) for observations and thinning of the data from every

second to every 20 s. A nonlinear least squares fit for a non-rectangular hyperbola was used to identify the net photosynthesis–photon flux density curve metrics (Marshall and Biscoe 1980). The model is as follows:

$$P_{\text{net}} = \frac{\Phi\text{PAR} + \sqrt{(\varphi\text{PPFD} + P_{\max})^2} - 4\Theta\varphi\text{PAR}P_{\max}}{2\Theta} - R_d, \quad (1)$$

where the parameters are P_{net} and $P_{\max}$ (area-based net and maximum gross photosynthetic rates, respectively), R_d (dark respiration), AQY (φ, apparent quantum yield), PAR (photosynthetically active radiation), and Theta (Θ, curvature parameter, dimensionless). I_k was calculated by dividing the $P_{\max}$ by the AQY, which was 384 µmol photons m^{-2} s^{-1} and there was no indication of photoinhibition (Fig. S2). Net photosynthetic rate was therefore measured at 451 ± 12 (mean ± SD from 10 light measurements) µmol photons m^{-2} s^{-1} to ensure that the experimental trials were run at saturating light conditions.

Acute thermal stress experiment to test thermal performance

Acute heat ramping experiments were used to assess net photosynthesis (n = 32) or dark respiration (n = 32) of replicate fragments from each coral colony. To measure net photosynthesis (NP) and dark respiration (R_d), coral fragments were placed in individual closed-system acrylic respiration chambers (650 ml) (Australian Institute of Marine Science, Townsville, Australia) with rotating stir bars (200 rpm) (Fig. 1j). Filtered (pore size ~ 100 µm) seawater was used for all experimental assays. Eight experimental coral fragments were moved from their ambient and nutrient-enriched seawater flow-through holding tanks (4 enriched and 4 control) and randomly assigned to one of the 10 respirometry chambers. Replicate seawater-only chambers were used as controls (n = 2) for background subtraction during each trial (n = 4 NP trials, n = 4 R_d trials). Each of the R_d heat ramping experiments began at approximately 05:30, and corals were kept in complete darkness by a black tarp cover and black trash bag covers on all windows or doors. The R_d corals were exposed to ten sequential temperatures (20, 22, 24, 28, 30, 32, 34, 36, 37, and 38 °C) for 20 min. Following the same experimental design, the light ramp trials began at approximately 13:00 and ended before sunset. During each light ramp trial, the coral fragments were exposed to nine sequential temperatures (20, 22, 24, 28, 30, 32, 34, 36, and 37 °C) for 20 min at saturating light. One less temperature ramp was required for the light trials because corals exhibited near zero oxygen production at 37 °C.

To maintain the assay temperature (± 0.1 °C), temperature was controlled in an insulated reservoir and holding tank using a thermostat system (Apex Controller, Neptune Systems, Morgan Hill, CA, USA) paired with aquarium heaters (Finnex 800 W Titanium Heater, Finnex 300 W Titanium Heater, Burnaby, British Columbia, Canada) and chillers (Aqua Logic Delta Star®, DS-4, San Diego, CA, USA). An air stone diffuser (Growneer, Shanghai, China) was added to the holding tank where the chambers were filled before each temperature ramp to provide circulation and oxygenation. Further, fresh seawater changes were conducted between each temperature ramp. Once the seawater in the insulated reservoir reached a stable temperature, the respirometry chambers containing both the coral fragments and controls were added and measurements started immediately. NP and R_d rates were quantified through oxygen production/consumption measured by fiber optic oxygen sensors using the same methods described above. Gross photosynthesis (GP) was calculated as NP plus R_d (as a positive value). After each incubation, we removed all coral tissue, dried the coral skeletons, and measured the surface area of each coral using the paraffin wax dipping technique described above to normalize the rates (µmol cm^{-2} h^{-1}) (Stimson and Kinzie III 1991; Veal et al. 2010).

Data analysis

Thermal performance curve characterization

Individual thermal performance curves (TPCs) for each of the biological rates of performance (µmol cm^{-2} h^{-1}) (GP and R_d) were fitted to the Sharpe–Schoolfield model (Sharpe and Demichele 1977; Schoolfield et al. 1981) using a nonlinear least squares regression (Table 1 lists the parameters and variables in this function).

$$\log(\text{rate})_i = b(T_c) + E_a\left(\frac{1}{T_c} - \frac{1}{\text{KT}_i}\right) - \log\left(1 + e^{E_h\left(\frac{1}{KT_h} - \frac{1}{KT_i}\right)}\right), \quad (2)$$

Fits were determined using the '*nls_multstart*' function in the '*nls.multstart*' package (Padfield and Matheson 2020) in R statistical software (v3.2.0) (R Core Team 2018, Padfield et al. 2015). The '*nls_multstart*' function allows for multiple starting values for each parameter and model selection is carried out using the Akaike information criterion (AIC) to identify the parameter set which best characterizes the data (Padfield et al. 2015). Random start parameter values are picked from a uniform distribution and the set with the lowest AIC value is retained (Padfield et al. 2015). The goodness of fit of the selected models was

Table 1 Parameters of the Sharpe–Schoolfield model using a nonlinear least squares regression

Parameter	Descriptions
$b(T_c)$	Log rate of metabolism normalized to a reference temperature (μmol cm^{-2} h^{-1})
E_a	Activation energy (electron volts, eV)
E_h	Temperature induced inactivation of enzyme kinetics past T_h for each population (electron volts, eV)
K	Boltzmann constant (8.62×10^{-5} eV K^{-1})
T_c	Reference temperature at which no low or high-temperature inactivation is experienced (defined here as 299.95 K or 26.8 °C)
T_h	Temperature (K) at which half the enzymes are inactivated
T_i	Temperature in Kelvin (K)
i	Individual coral fragment for each rate

examined both graphically and through computation of a pseudo-R^2 value (Padfield et al. 2015). Thermal performance metrics (acute thermal optimum (T_{opt}), maximal performance (μ_{max}), and rate of metabolism at a reference temperature ($b(T_c)$) were then determined from the TPCs (Fig. 4c–h). Acute T_{opt} and μ_{max} were calculated from the TPC parameters (Padfield et al. 2015), where acute T_{opt} is calculated as:

$$T_{\text{opt}} = \left(\frac{E_h \cdot T_h}{\left(E_h + \left(K \cdot T_h \cdot \log\left(\frac{E_h}{E_a} - 1 \right) \right) \right)} \right), \quad (3)$$

μ_{max} is the rate (either GP or R_d) at T_{opt} and $b(T_c)$ is the rate (either GP or R_d) at 26.8 °C (mean ambient seawater temperature conditions during the sampling period (October 1,2019, to October 26, 2019)) at the collection site obtained from the Mo'orea Coral Reef (MCR) Long Term Ecological Research Network (LTER) temperature time series (Leichter et al. 2019).

Statistical analysis

Two-sample Student's t-tests were used to test for differences in water column nutrient concentrations between the control and treatment sites. One PO_4^{3-} value was removed because it was below the detectable limit. Therefore, there was an n = 3 for the control water column PO_4^{3-} and DIN:DIP values. Individual general linear mixed effects models were run using the '*lme4*' package (Bates et al. 2015) in R for macroalgal % N, endosymbiont (chlorophyll *a* content (μg cm^{-2}), chlorophyll *a* content per cell (pg $cell^{-1}$), endosymbiont densities ($\times 10^6$ cells cm^{-2}), % N content (% of dry weight), N content $cell^{-1}$ (pg N $cell^{-1}$), coral response variables (tissue biomass (mg cm^{-2}), and % N content (% of dry weight)), and holobiont thermal response variables (T_{opt}, μ_{max}, and $b(T_c)$ for both GP and R_d). Treatment (control versus nutrient-enriched site) was a fixed effect and sampling block was included as a random effect in all models to account for block effects. Assumptions (i.e., normality, homogeneity of variance, and independence) were tested using the '*car*' package (Fox and Weisberg 2019) functions in R, and all assumptions were met.

ITS2 sequences were identified using the SymPortal analytical framework (symportal.org, Hume et al. 2019; supplemental file 1), and raw sequence data at NCBI under accession number PRJNA640364 (https://www.ncbi.nlm.nih.gov/bioproject/PRJNA640364/). The resulting counts matrix of Symbiodiniaceae profile names was analyzed for differences in community structure by treatment on Bray Curtis distance using the '*vegan*' package (Oksanen et al. 2013) in R, following calculation of sample relative abundances and square root transformation of the data. All data and code used for this study are available on GitHub (https://github.com/daniellembecker/Chronic_low_nutrient_enrichment_benefits_coral_thermal_performance_fore_reef_habitat) and at Zenodo (https://doi.org/10.5281/zenodo.5013256).

Results

Environmental variables

Quantifying nutrient regimes between enriched and control treatments

In the nutrient-enriched plots, *Lobophora variegata* % N, which is a proxy for nutrient levels over time, increased by an average of 11% ($p = 0.04$) (Fig. 2a) compared to the control treatment. In the water column above the nutrient-enriched plots $NO_2^- + NO_3^-$, PO_4^{3-}, and NH_4^+ all increased by an average of 0.14 μmol L^{-1} ($p < 0.01$) (Fig. 2c), 0.14 μmol L^{-1} ($p = 0.034$) (Fig. 2d), and 0.22 μmol L^{-1} ($p < 0.001$) (Fig. 2e) compared to the control treatment, respectively. There was no significant difference in water column DIN:DIP ratios ($p = 0.17$; Fig. 2f) or *L. variegata* carbon:nitrogen (C:N) ratios ($p = 0.76$; Fig. 2b) between the nutrient-enriched and control treatments. Our reported water column nutrient

measurements likely underestimate the actual concentrations seen by corals during the 15-month field exposure period because they were taken two months after the Osmocote® diffusers had been deployed (Burkepile et al. 2020).

Endosymbiont and coral response variables

Endosymbiont response variables

Several parameters associated with endosymbiont physiology were significantly affected by the 15-month nutrient enrichment period. Corals had significantly higher endosymbiont densities when enriched, with 54% more cells per cm^{-2} compared to controls ($F_{1,30} = 17.81$, $p < 0.001$; Fig. 3a, Table S1 in supplemental file 1). Endosymbiont N content $cell^{-1}$ (pg N $cell^{-1}$) was 44% higher in control corals compared to enriched corals ($F_{1,30} = 5.77$, $p = 0.02$; Fig. 3d, Table S1 in supplemental file 1). However, there was no significant difference in the total chlorophyll *a* content ($F_{1,6} = 1.78$, $p = 0.23$; Fig. 3b, Table S1 in supplemental file 1), chlorophyll *a* content per cell ($F_{1,6} = 1.40$, $p = 0.28$; Fig. 3c, Table 2.2), total % N content for algal endosymbionts under nutrient enrichment compared to the control ($F_{1,30} = 0.64$, $p = 0.43$; Fig. 3e, Table S1 in supplemental file 1), or C:N ratios for the

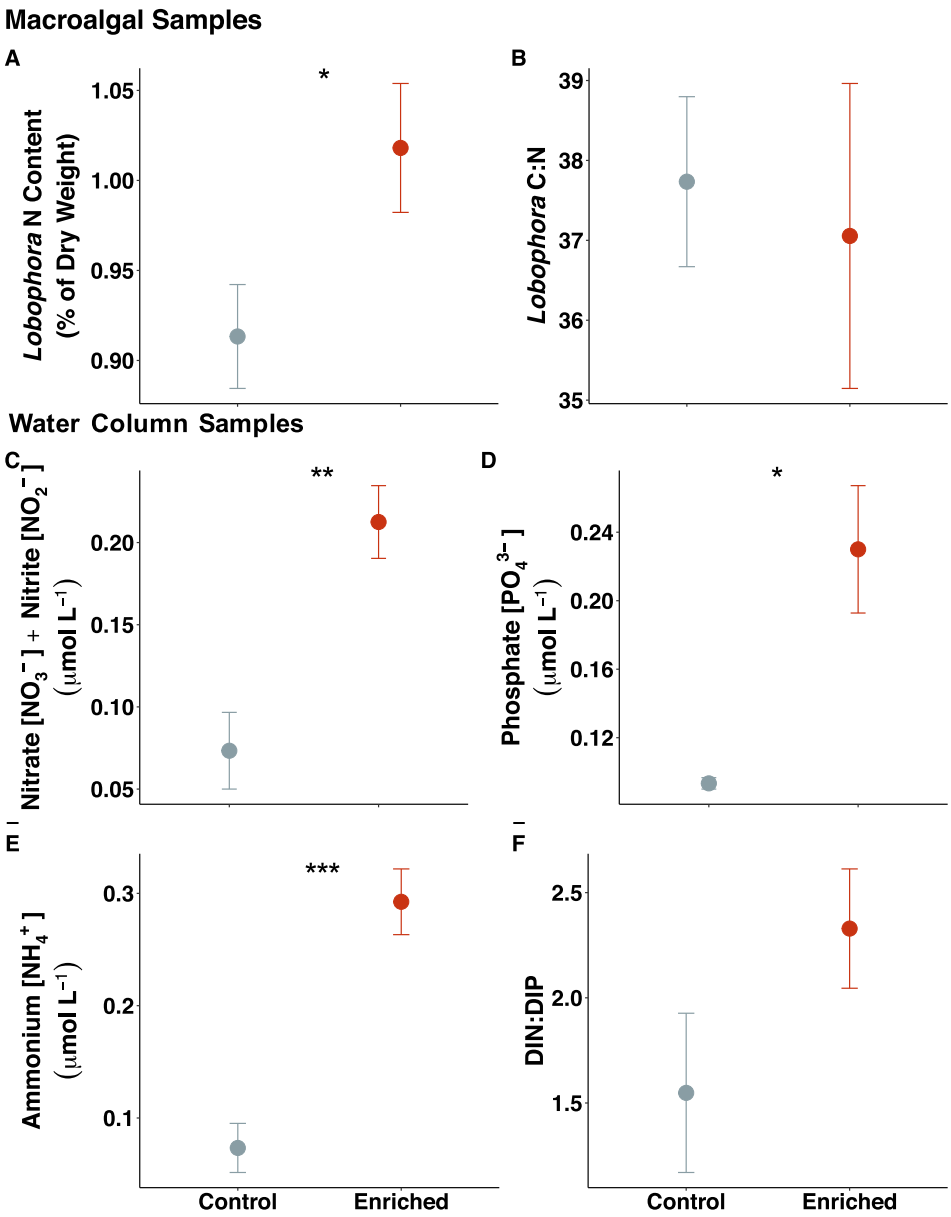

Fig. 2 Comparison of the **a** % nitrogen content of *Lobophora variegata*, **b** *L. variegata* C:N ratios, **c** water column nitrite (NO_2^-) + nitrate (NO_3^-) (µmol L^{-1}), **d** phosphate (PO_4^{3-}) (µmol L^{-1}), **e** ammonium (NH_4^+) (µmol L^{-1}), and **f** DIN:DIP ratios mean (± SE) values for each sample block ($n = 4$ per treatment, $n = 3$ for PO_4^{3-} and DIN:DIP, $n = 8$ per treatment for % nitrogen content and C:N) at the control and nutrient-enriched site on the north shore fore reef in Mo'orea, French Polynesia. Water column measurements (Fig. 2**c–f**) were taken at the end of the field experiment. Significance level is shown with asterisks (*p*-values < 0.05, < 0.01, and < 0.001 are *, **, and ***, respectively)

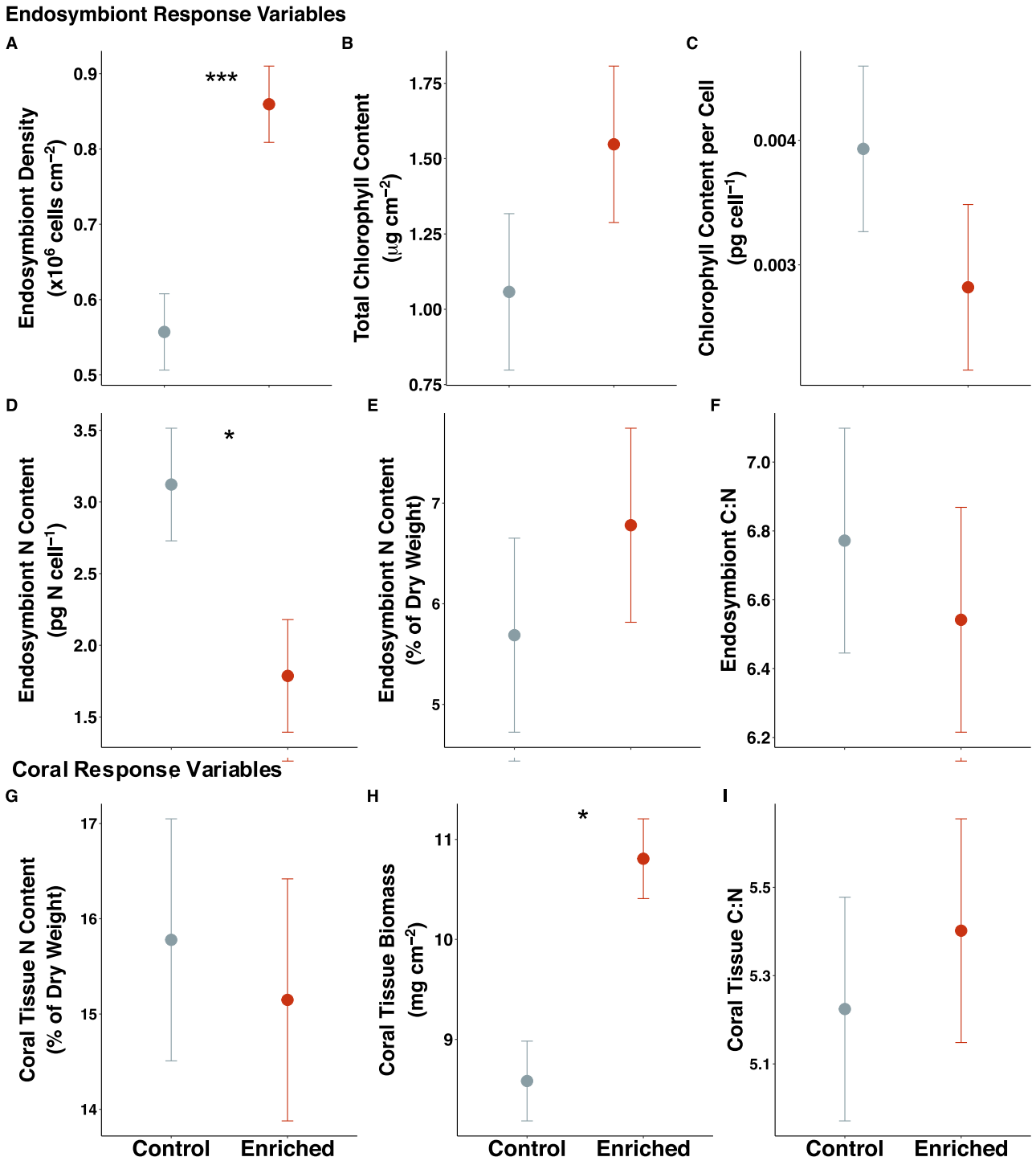

Fig. 3 Comparison of the **a** endosymbiont densities ($\times 10^6$ cells cm^{-2}), **b** chlorophyll *a* content (µg cm^{-2}), **c** chlorophyll *a* content per cell (pg $cell^{-1}$), **d** endosymbiont N content $cell^{-1}$ (pg N $cell^{-1}$), **e** endosymbiont % N content, **f** endosymbiont C:N ratios **g** coral tissue % N content, **h** tissue biomass (mg cm^{-2}), and **i** coral tissue C:N ratios mean (± SE) values extracted using the *'lsmeans'* function in R for all *Pocillopora* spp. coral fragments (n = 32) at the control and nutrient-enriched site on the north shore fore reef in Mo'orea, French Polynesia. Significance level is shown with asterisks (p-values < 0.05, < 0.01, and < 0.001 are *, **, and ***, respectively)

endosymbionts ($F_{1,6}$ = 0.25, p = 0.64; Fig. 3f, Table S2 in supplemental file 1). Sequencing of ITS2 resulted in 577,152 sequences total and a mean of 18,036 sequences per sample. Corals hosted predominantly *Cladocopium* spp. (ITS2 profile C42g.C42a.C42.2.C1.C1b.C42b. C42h; > 99%) based on SymPortal reference nomenclature

(Hume et al. 2019) with a few sequences of *Durusdinium* sp. (D1; ~ 0.05%), and no differences in ITS2 profiles between the two treatments ($p > 0.05$, Fig. S3 in supplemental file 1).

Coral response variables

For the coral response variables, the total tissue biomass (mg cm^{-2}) was 22% higher for the experimentally enriched corals compared to controls ($F_{1,6} = 15.52$, $p < 0.01$; Fig. 3h, Table S1 in supplemental file 1), but there was no difference in the tissue % N ($F_{1,6} = 0.12$, $p = 0.74$; Fig. 3g, Table S1 in supplemental file 1) or coral tissue C:N ratios ($F_{1,6} = 0.25$, $p = 0.64$; Fig. 3i, Table S2 in supplemental file 1) between nutrient-enriched corals and control corals.

Holobiont response variables

We found that nutrient enrichment generally increased metabolic responses of corals to acute thermal stress in terms of their measures of performance. Specifically, the nutrient-enriched treatment had μ_{max} (maximal rate of performance) GP rates that were 29% higher than the control colonies ($F_{1,6} = 26.86$, $p < 0.01$; Fig. 4c, Table S2 in supplemental file 1). There was also a 12% higher, but nonsignificant, μ_{max} for R_d rates in the nutrient-enriched corals compared to the controls ($F_{1,30} = 2.30$, $p = 0.14$; Fig. 4d, Table S2 in supplemental file 1). Similar trends were seen in the $b(T_c)$ (rate of metabolism at a reference temperature) results, with the nutrient-enriched treatment having 33% higher $b(T_c)$ for rates of GP ($F_{1,30} = 34.37$, $p < 0.001$; Fig. 4e, Table S2 in supplemental file 1) compared to the control colonies. There was also a 12% higher, but nonsignificant, $b(T_c)$ for R_d rates in the nutrient-enriched corals compared to the control colonies ($F_{1,30} = 2.38$, $p = 0.13$; Fig. 4f, Table S2 in supplemental file 1). There was no significant effect of treatment for the acute T_{opt} of GP rates ($F_{1,30} = 0.46$, $p = 0.50$; Fig. 4g, Table S2 in supplemental file 1) or R_d rates ($F_{1,6} = 0.18$, $p = 0.68$; Fig. 4h, Table S2 in supplemental file 1) in *Pocillopora* spp. colonies.

Discussion

Our study found that metabolic responses of the Pacific branching coral, *Pocillopora* spp., benefitted from a 15-month enrichment (3.4 × increase in N and 2.5 × increase in P) on a fore reef site in Mo'orea, French Polynesia. When enriched with nutrients, corals had significantly higher endosymbiont densities and total tissue biomass compared to controls. Further, corals that were enriched with nutrients exhibited higher gross photosynthetic maximal performance and rates of gross photosynthesis at a reference ambient temperature compared to unenriched corals. There was no difference in acute thermal optimum values between the two treatments. To our knowledge, this is the first study to show the effects of chronic nutrient enrichment on coral thermal performance in a fore reef habitat.

Explicit TPC approaches are historically rare for corals (but see, Jokiel and Coles 1977; Al-Horani 2005), but have been utilized more recently to quantify thermal sensitivity and instantaneous performance in response to environmental fluctuations (Aichelman et al. 2019; Jurriaans and Hoogenboom 2019; Silbiger et al. 2019; Becker and Silbiger 2020; Gould et al. 2021). TPC's are a valuable mechanistic approach to characterize thermal performance and thermal sensitivity trends across geographic ranges (Angilletta Jr. 2009; Sgrò et al. 2010; Jurriaans and Hoogenboom 2019; Kellermann et al. 2019; Silbiger et al. 2019), between ectothermic species (Dell et al. 2011; Sinclair et al. 2012; Bestion et al. 2018), and among populations and/or individuals (Huey and Kingsolver 1989; Knies et al. 2009). Further, TPC's provide insight into the interactive effects of temperature and other altered environmental conditions, such as nutrient enrichment and sedimentation (Bestion et al. 2018; Kellermann et al. 2019; Becker and Silbiger 2020).

Nutrient cycling within the coral holobiont—which includes the algal endosymbionts, microbial communities, and the coral host—is complex. Many studies have investigated the direct and indirect effects of nutrient enrichment on coral reef ecosystems and indicate that endosymbiont population densities are a key factor determining coral performance (Cunning and Baker 2013; Wiedenmann et al. 2013; D'Angelo and Wiedenmann 2014; Cunning et al. 2017; Rosset et al. 2017; Kitchen et al. 2020). A recent study showed that endosymbionts can alter their photophysiology to maintain coral productivity and host nutrition stability over a range of endosymbiont densities (Krueger et al. 2020). Our study found a trend of reduced nitrogen content per endosymbiont cell in the nutrient-enriched treatment coral colonies, indicating some form of competition for N, due to higher endosymbiont densities. The increased density of endosymbionts in the nutrient-enriched treatment may have led to the allocation of nitrogen to each individual cell to be less than the control treatment. We also observed lower C:N ratios in the coral host compared to algal endosymbionts—a similar trend to other published studies (Muller-Parker et al. 1994; Tanaka et al. 2018). Algal endosymbionts are thought to contribute to the dynamic N cycles occurring within the coral holobiont and are not N limited, but instead actively produce organic N that drives microscale N cycles within the system (Tanaka et al. 2018).

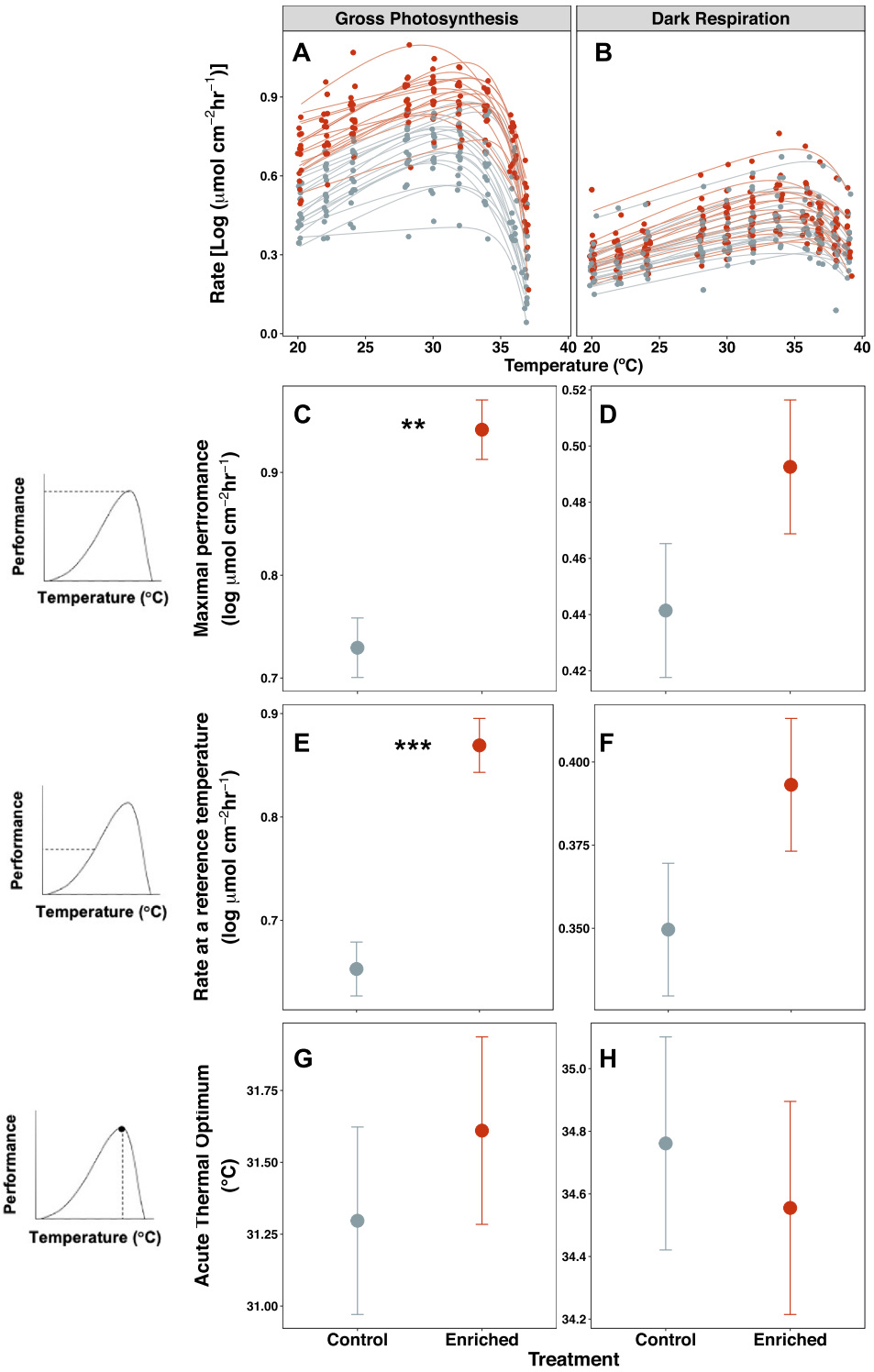

Fig. 4 Thermal performance curves (TPCs) of log (x + 1) fitted to the Sharpe–Schoolfield model (Sharpe and Demichele 1977; Schoolfield et al. 1981) using a nonlinear least squares regression **a** gross photosynthetic and **b** dark respiration rates (µmol cm^{-2} h^{-1}) from *Pocillopora* spp. coral fragments (n = 32) at the nutrient-enriched (red) and control (gray) site on the north shore fore reef in Mo'orea, French Polynesia. Comparison of the **c**,**d** maximal performance (μ_{max}), **e**,**f** rate of metabolism at a reference temperature ($b(T_c)$) (26.8 °C), and **g**,**h** acute thermal optimum (T_{opt}) (°C) mean (± SE) values extracted from the TPCs using the *'lsmeans'* function in R for all *Pocillopora* spp. coral fragments (n = 32) at the control and nutrient-enriched site and its effect on their gross photosynthetic and dark respiration rates. Significance level is shown with asterisks (p-values < 0.05, < 0.01, and < 0.001 are *, **, and ***, respectively)

The addition of phosphorus has been found to be beneficial to endosymbionts in low nutrient environments (Ezzat et al. 2016; Morris et al. 2019); therefore, the excess phosphorus from the Osmocote® enrichment could have supported the endosymbiont functionality even though reduced nitrogen between endosymbiont cells was observed. An increase in phosphate can lead to increased endosymbiont function (e.g., through stabilization of thylakoid membranes; Wiedenmann et al. 2013) under thermal stress, which is supported by our results of enhanced µmax

and rate of photosynthesis at a reference temperature in the enriched corals. The influx of phosphate relative to ambient seawater may have led to a more stable N:P ratio within the coral holobiont in our experimental nutrient enrichment treatment compared to controls, although we did not measure N:P ratios in the coral. While increased density of endosymbionts can provide nutritional benefits, competition for nitrogen can also arise between individual endosymbiont cells, due to reduced nitrogen assimilation and increased cell biomass, generating a negative feedback loop that can impact endosymbiont population growth (Krueger et al. 2020). Although we did not test for shifts in total bacterial abundance, nutrient enrichment has been shown to increase the proliferation of bacteria that can steal resources directly from the photosymbionts or indirectly from other members of the holobiont (Shaver et al. 2017; Klinges et al. 2019). Overall, nutrient cycling within the coral holobiont is determined in large part by endosymbiont population and microbiome community dynamics, which have a direct influence on holobiont performance.

Variable responses to thermal stress can be elicited by changes in symbiont physiology due to nutrient enrichment based on nutrient species (e.g., nitrogen, phosphate, nitrate, nitrite, ammonium). A balanced addition of nitrogen and phosphate (i.e., no change in the DIN:DIP) can increase endosymbiont densities and chlorophyll *a* concentrations in reef-building corals (Shantz and Burkepile 2014; Morris et al. 2019). Yet, differences in nutrient identity (phosphate, ammonium, nitrate, or nitrite) and source (e.g., fish excretions or anthropogenic nutrient) can lead to disparate responses in the relationship between endosymbiont densities and coral colony function (Shantz and Burkepile 2014; Morris et al. 2019). For example, nitrate enrichment to the scleractinian coral, *Stylophora pistillata*, in a low phosphate treatment (NO_3^-: PO_4^{3-} = 2.5 µM: 0.05 µM) decreased carbon fixation rates and carbon translocation ability compared to control conditions (N: PO_4^{3-} = 0.5 µM: 0.05 µM) (Ezzat et al. 2015). In comparison, an enrichment treatment replacing nitrate with ammonium (NH_4^+: PO_4^{3-} = 2.5 µM: 0.05 µM) increased endosymbiont densities and chlorophyll *a* concentrations, while also yielding higher carbon fixation rates and carbon translocation ability compared to the nitrate-enriched conditions (NO_3^-: PO_4^{3-} = 2.5 µM: 0.05 µM) (Ezzat et al. 2015), which can contribute to overall coral energetic status and growth (Ezzat et al. 2015). Further, when *Pocillopora damicornis* nubbins grown in a phosphate-enriched treatment were exposed to thermal stress (one week at 30 °C compared to the control at 25 °C), significantly higher carbon incorporation in tissues and carbon translocation rates at 30 °C demonstrated enhanced thermal tolerance of the phosphorus-enriched corals, compared to control corals (Ezzat et al. 2016). We found that corals under nutrient-enriched conditions had higher endosymbiont densities and total tissue biomass. This in turn, contributed to higher gross photosynthetic maximal performance rates, and rates of metabolism (i.e., photosynthesis and respiration) at an ambient temperature.

Many covarying environmental conditions (i.e., flow dynamics, light, temperature, salinity, sedimentation) can contribute to the spectrum of responses of corals to nutrient enrichment (Dubinsky and Stambler 1996; Fabricius 2005; Brodie et al. 2012; Humanes et al. 2017; Fisher et al. 2019). Alongshore and cross-reef transport on coral reef ecosystems like in Mo'orea, French Polynesia, is directly related to the physical constraints of temperature, water clarity, nutrient fluxes, coral larval recruitment, and disturbances that create contrasting reef environments (Leichter et al. 2013). The lagoonal habitats in Mo'orea, especially the fringing reefs, have higher retention times due to the topography of the reef habitat, which can lead to an increase in nitrate levels of $\sim$ 0.05–0.20 µmol L^{-1} higher than the fore reef (Leichter et al. 2013). The higher nutrient levels on the fringing reef along with increased sedimentation and reduced coral thermal performance were associated with reduced percent cover of *Pocillopora acuta* (Becker and Silbiger 2020). Conversely, fore reef environments in Mo'orea experience lower light levels, temperatures, sedimentation rates, and turbidity than the lagoon habitats (Leichter et al. 2013; Rivest and Hofmann 2014; Dubé et al. 2017; Carpenter 2018; Edmunds and Burgess 2018; Rivest et al. 2018). Our data show that corals on fore reefs may benefit from slight increases in nutrient concentrations ($\sim$ 1.58 µmol L^{-1} DIN + $\sim$ 0.64 µmol L^{-1} DIP), enhancing the physiological response of corals to thermal stress; highlighting that tracking nutrient conditions in less variable fore reef environments may be a key to understanding and forecasting the response of corals to warming events across reef habitats.

As coral reef environments are highly variable, different nutrient regimes can elicit a range of responses from corals. Gil (2013) proposed that underlying nonlinear (i.e., unimodal) relationships between corals and nutrient concentrations could explain the heterogeneous responses (e.g., positive, negative, or neutral) exhibited in many case studies. For example, *Porites* spp. growth rate exhibited a unimodal (i.e., nonlinear, single peak) response to increasing effective nutrient enrichment (0, 5, 10, 25, 50, 85, or 125 g of an Osmocote® slow release garden fertilizer (19:6:12, N:P:K) (Barboza et al. 2008; Gil 2013). Further, corals found in environments with sub-optimal or low nutrient levels, have been shown to exhibit increased performance in thermally stressed environments (Dunn et al. 2012; D'Angelo and Wiedenmann 2014). Yet, a shift to higher nutrient concentrations in the reef environment

can increase corals susceptibility to heat stress (D'Angelo and Wiedenmann 2014; Vega Thurber et al. 2014). Overall, unimodal projections of nutrient enrichment suggest that low to moderate levels of nutrients could be beneficial to corals, while higher nutrient levels are detrimental under certain conditions. Many coral nutrient laboratory studies use high nutrient concentrations that are not typically experienced in reef environments, making it difficult to understand how corals respond to nutrients in nature (Szmant 2002; Fabricius 2005; Le Grand and Fabricius 2011). In the current study, the enrichment for all nutrient species was low to moderate relative to ambient seawater ($\sim$ 1.58 µmol L^{-1} increase in total $NO_3^- + NO_2^-$, and NH_4^+ and $\sim$ 0.64 µmol L^{-1} increase in PO_3^{4-}), which could explain the positive effect of nutrient enrichment on coral thermal performance.

Many coral populations host a diverse assemblage of endosymbiont species that exhibit differential performance and physiological responses to environmental variability (Rowan 2004; Cunning and Baker 2013). For example, the Symbiodiniaceae species, *Durusdinium trenchii,* have been shown to remain associated with the coral host, retain photosynthetic function, and increase host survival when encountering acute thermal anomalies (Jones et al. 2008; Silverstein et al. 2015; Bay et al. 2016). In contrast, more thermally sensitive symbionts found in the genus *Cladocopium* have been associated with higher coral growth rates due to their ability to translocate higher amounts of carbon-based energy to the coral host compared to *Durusdinium* species (Cantin et al. 2009; Jones and Berkelmans 2010). While one endosymbiont type is usually dominant in an individual coral colony (Silverstein et al. 2012), there could be a shift in the relative abundance of symbionts (i.e., 'shuffling') in response to shifting environmental conditions (Jones et al. 2008; Reich et al. 2017), as some Symbiodiniaceae species perform better under certain environmental conditions. Performance results may then be explained not by acclimatization of existing communities, but by symbiont community shifts. In this study, there was no difference in symbiont type between the nutrient-enriched treatment and controls on the fore reef. The dominant symbiont type found in all corals was C42, a symbiont type in the *Cladocopium* genus, confirming that endosymbiont type was not a factor influencing the physiological responses to thermal stress of the coral hosts between the nutrient-enriched treatment and controls on the fore reef.

There are some limitations that should be considered when interpreting our results. Six months prior to our experiment, corals in Mo'orea experienced a major bleaching event from $\sim$ March to July 2019 (Burgess et al. 2021), which could have affected the results. Sub-lethal bleaching events can lead to increased survival after subsequent stress events (Ainsworth et al. 2016); therefore, the corals in this experiment may have acquired some resistance to temperature stress as a result of the recent bleaching event. The impacts of the March to July 2019 bleaching event in Mo'orea are still being gathered and analyzed, but from preliminary analyses from this experiment, there did not appear to be any differential bleaching between our treatment and control groups. Importantly, our thermal performance curves were acute heating events. Acute TPCs are commonly used for comparative thermal physiology across differing environmental conditions (Angilletta Jr. 2009; Dell et al. 2013; Aichelman et al. 2019), but do not represent the absolute temperatures corals could withstand in a more sustained heating event, like a prolonged bleaching episode. Further, while morphological characteristics were used to identify the corals used in this study (Maté et al. 2016), similar *Pocillopora* spp. may be cryptic and represent distinct genetic linkages making them morphologically indistinguishable (Johnston et al. 2018; Burgess et al. 2021). As studies have found that corals can exhibit intraspecific variation in their responses to thermal stress (Edmunds 1994; D'Croz and Maté 2004; Weis 2010; Silbiger et al. 2019), if multiple coral haplotypes were present in our study there may have been impacts on the variation we saw in performance between or within treatments. However, even with these potential limitations, our study shows that chronic nutrient enrichment on a fore reef habitat can be beneficial to the thermal performance of corals.

Understanding the effect of nutrient inputs on the physiological response of corals to temperature is essential over various environmental conditions to predict how local anthropogenic stressors and oceanographic conditions (i.e., upwelling, and internal waves) affect coral reef ecosystems. Here, we showed the effects of a chronic in situ nutrient enrichment experiment on the thermal performance of a Pacific branching coral species. While there was no difference in the acute T_{opt} between corals from ambient sites and those from enriched sites, nutrient-enriched corals exhibited shifts in the shape of their TPCs, with higher maximal performance and rates of metabolism at an ambient temperature for their gross photosynthetic rates. As environmental degradation from anthropogenic stressors becomes more prominent on coral reef ecosystems, understanding how nutrient dynamics influence the thermal performance of corals across geographic ranges, environmental variability, and natural nutrient flux, and a variety of reef habitats will help inform research-based management decisions for reefs at risk.

Supplementary information The online version contains supplementary material available at https://doi.org/10.1007/s00338-021-02138-2.

Acknowledgements We thank the Mo'orea Coral Reef Long-term Ecological Research Network, the University of California, Berkeley Richard B. Gump South Pacific Research Station, the University of California, Santa Barbara Marine Science Institutes Analytical Lab, and California State University, Northridge, for facilities support. Special thanks to J. Rosales and K. Speare for their support and dedication in collecting data in the field, as well the numerous individuals who contributed to the establishment and maintenance of the enrichment experiment on the forereef. We thank Dr. Marie Strader for the acquisition of the experimental tank temperature data. Additionally, thanks to Dr. P. J. Edmunds and Dr. R. C. Carpenter for their guidance and support. This research was funded in part by California State University, Northridge (CSUN) to NJS, US National Science Foundation OCE#19-24281 to NJS and Emerging Frontiers 1921465 to HMP, CSUN Office of Graduate Studies, Department of Biology, Associated Students, College of Sciences and Mathematics, and Research and Graduate Studies to DMB, and the National Science Foundation 2019 Graduate Research Fellowship to DMB. Funds to conduct the enrichment study were also provided by National Science Foundation Biological Oceanography Grants # 1442306 and #1635913 to RVT and 1547952 to DEB. Material are also supported by the US National Science Foundation under Grant (OCE#16-37396), as well as a generous gift from the Gordon and Betty Moore Foundation. This work represents a contribution of the Mo'orea Coral Reef (MCR) LTER Site and is CSUN Marine Biology contribution #322. Research was completed under permits issued by the French Polynesian Government (De´le´gation a'la Recherche) and the Haut-commissariat de la Re´publique en Polyne´sie Francaise (DTRT) (Protocole d'Accueil 2005-2019). We acknowledge that our research was completed on the unceded land of the Mā'ohi peoples, we honor and acknowledge the Mā'ohi community, their elders both past and present, as well as future generations.

Declarations

Conflict of interest On behalf of all authors, the corresponding author states there is no conflict of interest.

References

Aichelman HE, Zimmerman RC, Barshis DJ (2019) Adaptive signatures in thermal performance of the temperate coral *Astrangia poculata*. J Exp Biol jeb.189225

Ainsworth TD, Heron SF, Ortiz JC, Mumby PJ, Grech A, Ogawa D, Eakin CM, Leggat W (2016) Climate change disables coral bleaching protection on the Great Barrier Reef. Science (80) 352:338–342

Al-Horani FA (2005) Effects of changing seawater temperature on photosynthesis and calcification in the scleractinian coral *Galaxea fascicularis*, measured with O2, Ca2+ and pH microsensors. Sci Mar 69:347–354

Allgeier JE, Valdivia A, Cox C, Layman CA (2016) Fishing down nutrients on coral reefs. Nat Commun 7:1–5

Andrews RM, Schwarzkopf L (2012) Thermal performance of squamate embryos with respect to climate, adult life history, and phylogeny. Biol J Linn Soc 106:851–864

Angilletta Jr. MJ (2009) Thermal Adaptation: a Theoretical and Empirical Synthesis. Oxford University Press.

Barboza PS, Parker KL, Hume ID (2008) Integrative wildlife nutrition. Springer Science & Business Media.

Bassim KM, Sammarco PW (2003) Effects of temperature and ammonium on larval development and survivorship in a scleractinian coral (*Diploria strigosa*). Mar Biol 142:241–252

Bates D, Mächler M, Bolker BM, Walker SC (2015) Fitting linear mixed-effects models using lme4. *arXiv preprint* arXiv:1406.5823.

Bay LK, Doyle J, Logan M, Berkelmans R (2016) Recovery from bleaching is mediated by threshold densities of background thermo-tolerant symbiont types in a reef-building coral. R Soc Open Sci 3:160322

Becker DM, Silbiger NJ (2020) Nutrient and sediment loading affect multiple facets of functionality in a tropical branching coral. J Exp Biol 223

Bestion E, Schaum C-E, Yvon-Durocher G (2018) Nutrient limitation constrains thermal tolerance in freshwater phytoplankton. Limnol Oceanogr Lett 3:436–443

Bongiorni L, Shafir S, Angel D, Rinkevich B (2003) Survival, growth and gonad development of two hermatypic corals subjected to in situ fish-farm nutrient enrichment. Mar Ecol Prog Ser 253:137–144

Brander LM, Eppink F V., Schägner P, van Beukering PJH, and Wagtendonk A (2015) GIS-based mapping of ecosystem services: The case of coral reefs. Benefit Transfer of Environmental and Resource Values. Springer, Dordrecht., pp 465–485

Brodie JE, Kroon FJ, Schaffelke B, Wolanski EC, Lewis SE, Devlin MJ, Bohnet IC, Bainbridge ZT, Waterhouse J, Davis AM (2012) Terrestrial pollutant runoff to the Great Barrier Reef: An update of issues, priorities and management responses. Mar Pollut Bull 65:81–100

Burgess, S. C., Johnston, E. C., Wyatt, A. S., Leichter, J. J., & Edmunds, P. J. (2021). Response diversity in corals: hidden differences in bleaching mortality among cryptic *Pocillopora* species. *Ecology*, e03324

Burkepile DE, Hay ME (2009) Nutrient versus herbivore control of macroalgal community development and coral growth on a Caribbean reef. Mar Ecol Prog Ser 389:71–84

Burkepile DE, Shantz AA, Adam TC, Munsterman KS, Speare KE, Ladd MC, Rice MM, Ezzat L, McIlroy S, Wong JCY, Baker DM, Brooks AJ, Schmitt RJ, Holbrook SJ (2020) Nitrogen Identity Drives Differential Impacts of Nutrients on Coral Bleaching and Mortality. Ecosystems 23:798–811

Cantin NE, Van Oppen MJH, Willis BL, Mieog JC, Negri AP (2009) Juvenile corals can acquire more carbon from high-performance algal symbionts. Coral Reefs 28:405–414

Carpenter R (2018) Time Series | Moorea Coral Reef LTER.

Carpenter R (2019) MCR LTER: Coral Reef: Benthic Photosynthetically Active Radiation (PAR), ongoing since 2009. Moorea Coral Reef LTER knb-lter-mcr.4005.10

Charpy L, Casareto BE, Langlade MJ, Suzuki Y (2012) Cyanobacteria in Coral Reef Ecosystems: A Review. J Mar Biol 2012:1–9

Cisneros-Montemayor AM, Sumaila UR (2010) A global estimate of benefits from ecosystem-based marine recreation: potential impacts and implications for management. J Bioeconomics 12:245–268

Comeau S, Carpenter RC, Edmunds PJ (2013) Effects of feeding and light intensity on the response of the coral *Porites rus* to ocean acidification. Mar Biol 160:1127–1134

Comeau S, Carpenter RC, Edmunds PJ (2014) Effects of irradiance on the response of the coral *Acropora pulchra* and the calcifying alga *Hydrolithon reinboldii* to temperature elevation and ocean acidification. J Exp Mar Bio Ecol 453:28–35

Cunning R, Baker AC (2013) Excess algal symbionts increase the susceptibility of reef corals to bleaching. Nat Clim Chang 3:259–262

Cunning R, Muller EB, Gates RD, Nisbet RM (2017) A dynamic bioenergetic model for coral-Symbiodinium symbioses and coral bleaching as an alternate stable state. J Theor Biol 431:49–62

D'Angelo C, Wiedenmann J (2014) Impacts of nutrient enrichment on coral reefs: New perspectives and implications for coastal

management and reef survival. Curr Opin Environ Sustain 7:82–93

D'Croz L, Maté JL (2004) Experimental responses to elevated water temperature in genotypes of the reef coral *Pocillopora damicornis* from upwelling and non-upwelling environments in Panama. Coral Reefs 23:473–483

D'Croz L, Maté JL, Oke JE (2001) Responses to elevated sea water temperature and UV radiation in the coral *Porites lobata* from upwelling and non-upwelling environments on the Pacific coast of Panama. Bull Mar Sci 69:203–214

Dell AI, Pawar S, Savage VM (2011) Systematic variation in the temperature dependence of physiological and ecological traits. Proc Natl Acad Sci U S A 108:10591–10596

Dell AI, Pawar S, Savage VM (2013) The thermal dependence of biological traits. Ecology 94:1205–1206

Dubé CE, Mercière A, Vermeij MJA, Planes S (2017) Population structure of the hydrocoral *Millepora platyphylla* in habitats experiencing different flow regimes in Moorea, French polynesia. PLoS One 12:1–20

Dubinsky Z, Stambler N (1996) Marine pollution and coral reefs. Glob Chang Biol 2:511–526

Dunn JG, Sammarco PW, LaFleur G (2012) Effects of phosphate on growth and skeletal density in the scleractinian coral *Acropora muricata*: A controlled experimental approach. J Exp Mar Bio Ecol 411:34–44

Edmunds PJ (1994) Evidence that reef-wide patterns of coral bleaching may be the result of the distribution of bleaching-susceptible clones. Mar Biol 121:137–142

Edmunds PJ, Burgess SC (2018) Correction: Size-dependent physiological responses of the branching coral *Pocillopora verrucosa* to elevated temperature and PCO2. J Exp Biol 221:3896–3906

Ezzat L, Maguer JF, Grover R, Ferrier-Pagés C (2015) New insights into carbon acquisition and exchanges within the coral–dinoflagellate symbiosis under NH4+ and NO3- supply. Proc R Soc B Biol Sci 282:

Ezzat L, Maguer JF, Grover R, Ferrier-Pagès C (2016) Limited phosphorus availability is the Achilles heel of tropical reef corals in a warming ocean. Sci Rep 6:1–11

Fabricius KE (2005) Effects of terrestrial runoff on the ecology of corals and coral reefs: Review and synthesis. Mar Pollut Bull 50:125–146

Fernandes L, Marangoni DB, Pagès CF, Rottier C, Bianchini A, Grover R (2020) Unravelling the different causes of nitrate and ammonium effects on coral bleaching. Sci Rep 1–14

Fisher R, Bessell-Browne P, Jones R (2019) Synergistic and antagonistic impacts of suspended sediments and thermal stress on corals. Nat Commun 10:1–9

Fong P, Donohoe RM, Zedler JB (1994) Nutrient concentration in tissue of the macroalga *Enteromorpha* as a function of nutrient history: an experimental evaluation using field microcosms. 106:273–281

Fox J, Weisberg S (2019) An R companion to applied regression (Third). Thousand Oaks CA: Sage,

Gil MA (2013) Unity through nonlinearity: A unimodal coral-nutrient interaction. Ecology 94:1871–1877

Gould K, Bruno JF, Ju R, Goodbody-Gringley G (2021) Upper-mesophotic and shallow reef corals exhibit similar thermal tolerance, sensitivity and optima. Coral Reefs 40:907–920

Le Grand HM, Fabricius KE (2011) Relationship of internal macrobioeroder densities in living massive *Porites* to turbidity and chlorophyll on the Australian Great Barrier Reef. Coral Reefs 30:97–107

Griffiths JS, Pan TCF, Kelly MW (2019) Differential responses to ocean acidification between populations of *Balanophyllia elegans* corals from high and low upwelling environments. Mol Ecol 28:2715–2730

Halpern BS, Frazier M, Potapenko J, Casey KS, Koenig K, Longo C, Lowndes JS, Rockwood RC, Selig ER, Selkoe KA, Walbridge S (2015) Spatial and temporal changes in cumulative human impacts on the world's ocean. Nat Commun 6:1–7

Howells EJ, Bauman AG, Vaughan GO, Hume BCC, Voolstra CR, Burt JA (2020) Corals in the hottest reefs in the world exhibit symbiont fidelity not flexibility. Mol Ecol 29:899–911

Huey RB, Kingsolver JG (1989) Evolution of thermal sensitivity of ectotherm performance. Trends Ecol Evol 4:131–135

Hughes TP, Anderson KD, Connolly SR, Heron SF, Kerry JT, Lough JM, Baird AH, Baum JK, Berumen ML, Bridge TC, Claar DC, Eakin CM, Gilmour JP, Graham NAJ, Harrison H, Hobbs JPA, Hoey AS, Hoogenboom M, Lowe RJ, McCulloch MT, Pandolfi JM, Pratchett M, Schoepf V, Torda G, Wilson SK (2018) Spatial and temporal patterns of mass bleaching of corals in the Anthropocene. Science 359:80–83

Hughes TP, Baird AH, Bellwood DR, Card M, Connolly SR, Folke C, Grosberg R, Hoegh-Guldberg O, Jackson JBC, Kleypas J, Lough JM, Marshall P, Nyström M, Palumbi SR, Pandolfi JM, Rosen B, Roughgarden J (2003) Climate change, human impacts, and the resilience of coral reefs. Science (80-) 301:929–933

Humanes A, Ricardo GF, Willis BL, Fabricius KE, Negri AP (2017) Cumulative effects of suspended sediments, organic nutrients and temperature stress on early life history stages of the coral *Acropora tenuis*. Sci Rep 7:44101

Hume BCC, Smith EG, Ziegler M, Warrington HJM, Burt JA, LaJeunesse TC, Wiedenmann J, Voolstra CR (2019) SymPortal: A novel analytical framework and platform for coral algal symbiont next-generation sequencing ITS2 profiling. Mol Ecol Resour 19:1063–1080

Jeffrey SW, Humphrey GF (1975) New spectrophotometric equations for determining chlorophylls a, b, c1 and c2 in higher plants, algae and natural phytoplankton. Biochem Physiol Pflanz 167:191–194

Johnson KS, Petty RL, Thomsen J (1985) Flow-Injection Analysis for Seawater Micronutrients. Adv Chem 7–30

Johnston EC, Forsman ZH, Toonen RJ (2018) A simple molecular technique for distinguishing species reveals frequent misidentification of Hawaiian corals in the genus *Pocillopora*. PeerJ 1:1–14

Jokiel PL, Coles SL (1977) Effects of Temperature on the Mortality and Growth of Hawaiian Rccf Corals. Mar Biol 43:201–208

Jones A, Berkelmans R (2010) Potential costs of acclimatization to a warmer climate: Growth of a reef coral with heat tolerant vs. sensitive symbiont types. PLoS One 5:e10437

Jones AM, Berkelmans R, Van Oppen MJH, Mieog JC, Sinclair W (2008) A community change in the algal endosymbionts of a scleractinian coral following a natural bleaching event: Field evidence of acclimatization. Proc R Soc B Biol Sci 275:1359–1365

Jurriaans S, Hoogenboom MO (2019) Thermal performance of scleractinian corals along a latitudinal gradient on the Great Barrier Reef. Philos Trans R Soc B Biol Sci 374:20180546

Kayanne H, Hirota M, Yamamuro M, Koike I (2005) Nitrogen fixation of filamentous cyanobacteria in a coral reef measured using three different methods. Coral Reefs 24:197–200

Kellermann V, Chown SL, Schou MF, Aitkenhead I, Janion-Scheepers C, Clemson A, Scott MT, Sgrò CM (2019) Comparing thermal performance curves across traits: How consistent are they? J Exp Biol 222: 11

Kinzie RA, Takayama M, Santos SR, Alice M, Iii RAK, Takayama L, Santos SR, Coffroth MA (2018) The Adaptive Bleaching Hypothesis: Experimental Tests of Critical Assumptions The Adaptive Bleaching Hypothesis: Experimental Tests of Critical Assumptions. 200:51–58

Kitchen RM, Piscetta M, Rocha M (2020) Symbiont transmission and reproductive mode influence responses of three Hawaiian coral larvae to elevated temperature and nutrients. Coral Reefs 1–13

Klinges JG, Rosales SM, McMinds R, Shaver EC, Shantz AA, Peters EC, Eitel M, Wörheide G, Sharp KH, Burkepile DE, Silliman BR, Vega Thurber RL (2019) Phylogenetic, genomic, and biogeographic characterization of a novel and ubiquitous marine invertebrate-associated Rickettsiales parasite, *Candidatus Aquarickettsia rohweri*, gen. nov., sp. nov. ISME J 13:2938–2953

Knies JL, Kingsolver JG, Burch CL (2009) Hotter is better and broader: Thermal sensitivity of fitness in a population of bacteriophages. Am Nat 173:419–430

Koop K, Booth D, Broadbent A, Brodie J, Bucher D, Capone D, Coll J, Dennison W, Erdmann M, Harrison P, Hoegh-Guldberg O, Hutchings P, Jones GB, Larkum AWD, O'Neil J, Steven A, Tentori E, Ward S, Williamson J, Yellowlees D (2001) ENCORE: The effect of nutrient enrichment on coral reefs. Synthesis of results and conclusions. Mar Pollut Bull 42:91–120

Krueger T, Horwitz N, Bodin J, Giovani M, Escrig S, Fine M, Meibom A, Krueger T (2020) Intracellular competition for nitrogen controls dinoflagellate population density in corals. Proc R Soc B Biol Sci 1922: 287

LaJeunesse TC, Parkinson JE, Gabrielson PW, Jeong HJ, Reimer JD, Voolstra CR, Santos SR (2018) Systematic Revision of Symbiodiniaceae Highlights the Antiquity and Diversity of Coral Endosymbionts. Curr Biol 28:2570-2580.e6

van de Leemput IA, Morrison TH, Kleypas J, van Nes EH, Barnes ML, Lough JM, Scheffer M, Hughes TP, Jackson JBC, Cumming GS, Cinner JE, Palumbi SR, Bellwood DR (2017) Coral reefs in the Anthropocene. Nature 546:82–90

Leichter J, Alldredge A, Bernardi G, Brooks A, Carlson C, Carpenter R, Edmunds P, Fewings M, Hanson K, Hench J, Holbrook S, Nelson C, Schmitt R, Toonen R, Washburn L, Wyatt A (2013) Biological and Physical Interactions on a Tropical Island Coral Reef: Transport and Retention Processes on Moorea, French Polynesia. Oceanography 26:52–63

Leichter J, Seydel K, Gotschalk C (2019) MCR LTER: Coral Reef: Benthic Water Temperature, ongoing since 2005. Moorea Coral Reef LTER

Leichter JJ, Genovese SJ (2006) Intermittent upwelling and subsidized growth of the scleractinian coral *Madracis mirabilis* on the deep fore-reef slope of Discovery Bay, Jamaica. Mar Ecol Prog Ser 316:95–103

Lin DT, Fong P (2008) Macroalgal bioindicators (growth, tissue N, d15N) detect nutrient enrichment from shrimp farm effluent entering Opunohu Bay, Moorea, French Polynesia. 56:245–249

Maier C, Weinbauer MG, Pätzold J (2010) Stable isotopes reveal limitations in C and N assimilation in the caribbean reef corals *Madracis auretenra*, *M. carmabi* and *M. formosa*. Mar Ecol Prog Ser 412:103–112

Marshall B, Biscoe P V (1980) A Model for C 3 Leaves Describing the Dependence of Net Photosynthesis on Irradiance. 31:29–39

Maté JL, Brandt M, Grassian B, Chiriboga Á (2016) Field Guide to Select Eastern Pacific Corals and Associated Coral Reef Biota. 593–637

Mayfield AB, Fan TY, Chen CS (2013) Physiological acclimation to elevated temperature in a reef-building coral from an upwelling environment. Coral Reefs 32:909–921

McClanahan TR, Sala E, Stickels PA, Cokos BA, Baker AC, Starger CJ, Jones IV SH (2003) Interaction between nutrients and herbivory in controlling algal communities and coral condition on Glover's Reef, Belize. Mar Ecol Prog Ser 261:135–147

McDevitt-Irwin JM, Baum JK, Garren M, Vega Thurber RL (2017) Responses of coral-associated bacterial communities to local and global stressors. Front Mar Sci 4:1–16

Monismith SG (2007) Hydrodynamics of Coral Reefs. Annu Rev Fluid Mech 39:37–55

Morris LA, Voolstra CR, Quigley KM, Bourne DG, Bay LK (2019) Nutrient availability and metabolism affect the stability of coral – Symbiodiniaceae symbioses. Trends Microbiol 27:678–689

Muller-Parker G, Cook CB, D'Ella CF (1994) Elemental composition ofthe coral *Pocillopora damicornis* exposed to elevated seawater ammonium. Pacific Sci 48:234–246

Muscatine L, Falkowski PG, Dubinsky Z, Cook PA, McCloskey LR (1989) The effect of external nutrient resources on the population dynamics of zooxanthellae in a reef coral. Proc R Soc London 236:311–324

Muscatine L, Falkowski PG, Porter JW, Dubinsky Z (1984) Fate of photosynthetic fixed carbon in light- and shade-adapted colonies of the symbiotic coral *Stylophora pistillata*. Proc R Soc London Ser B Biol Sci 222.1227:181–202

Nordemar I, Nyström M, Dizon R (2003) Effects of elevated seawater temperature and nitrate enrichment on the branching coral *Porites cylindrica* in the absence of particulate food. Mar Biol 142:669–677

O'Neil JM, Capone DG (2008) Nitrogen Cycling in Coral Reef Environments. Nitrogen Mar Environ 949–989

Oksanen J, Blanchet FG, Kindt R, Legendre P, Minchin PR, O'hara RB, Simpson GL, Solymos P, Stevens MHH, Wagner H (2013) vegan: Community Ecology Package. R Packag version 2–0

Olito C, White CR, Marshall DJ, Barneche DR (2017) Estimating monotonic rates from biological data using local linear regression. J Exp Biol 220:759–764

Padfield D, Matheson G (2020) nls.multstart: Robust Non-Linear Regression using AIC Scores. R Packag version 110

Padfield D, Yvon-Durocher G, Buckling A, Jennings S, Yvon-Durocher G (2015) Rapid evolution of metabolic traits explains thermal adaptation in phytoplankton. Ecol Lett 19: 133–142

Radice VZ, Hoegh-Guldberg O, Fry B, Fox MD, Dove SG (2019) Upwelling as the major source of nitrogen for shallow and deep reef-building corals across an oceanic atoll system. Funct Ecol 1–15

Reich HG, Robertson DL, Goodbody-Gringley G (2017) Do the shuffle: Changes in Symbiodinium consortia throughout juvenile coral development. PLoS One 12:1–18

Riegl B, Piller WE (2003) Possible refugia for reefs in times of environmental stress. Int J Earth Sci 92:520–531

Rivest EB, Hofmann GE (2014) Responses of the metabolism of the larvae of *Pocillopora damicornis* to ocean acidification and warming. PLoS One 9:e96172

Rivest EB, Kelly MW, DeBiasse MB, Hofmann GE (2018) Host and Symbionts in *Pocillopora damicornis* Larvae Display Different Transcriptomic Responses to Ocean Acidification and Warming. Front Mar Sci 5:186

Rogers CS (1990) Responses of coral reefs and reef organisms to sedimentation. Mar Ecol Prog Ser 62:185–202

Rosset S, Wiedenmann J, Reed AJ, D'Angelo C (2017) Phosphate deficiency promotes coral bleaching and is reflected by the ultrastructure of symbiotic dinoflagellates. Mar Pollut Bull 118:180–187

Rowan R (2004) Thermal adaptation in reef coral symbionts. Nature 430:742

Schlöder C, D'Croz L (2004) Responses of massive and branching coral species to the combined effects of water temperature and nitrate enrichment. J Exp Mar Bio Ecol 313:255–268

Schoolfield RM, Sharpe PJ, Magnuson CE (1981) Non-linear regression of biological temperature-dependent rate models based on absolute reaction-rate theory. J Theor Biol 88:719–719

Schulte PM, Healy TM, Fangue NA (2011) Thermal performance curves, phenotypic plasticity, and the time scales of temperature exposure. Integr Comp Biol 51:691–702

Serrano XM, Miller MW, Hendee JC, Jensen BA, Gapayao JZ, Pasparakis C, Grosell M, Baker AC (2018) Effects of thermal stress and nitrate enrichment on the larval performance of two Caribbean reef corals. Coral Reefs 37:173–182

Sgrò CM, Overgaard J, Kristensen TN, Mitchell KA, Cockerell FE, Hoffmann AA (2010) A comprehensive assessment of geographic variation in heat tolerance and hardening capacity in populations of *Drosophila melanogaster* from Eastern Australia. J Evol Biol 23:2484–2493

Shantz AA, Burkepile DE (2014) Context-dependent effects of nutrient loading on the coral-algal mutualism. Ecology 95:1995–2005

Sharpe PJH, Demichele DW (1977) Reaction-Kinetics of Poikilotherm Development. J Theor Biol 64:649–670

Shaver EC, Shantz AA, McMinds R, Burkepile DE, Thurber RLV, Silliman BR (2017) Effects of predation and nutrient enrichment on the success and microbiome of a foundational coral. Ecology 98:830–839

Shea F, Watts CE (1939) Dumas method for organic nitrogen. Ind Eng Chem Anal Ed 11 (6):333–334

Silbiger NJ, Goodbody G, John G, Hollie FB (2019) Comparative thermal performance of the reef-building coral *Orbicella franksi* at its latitudinal range limits. Mar Biol 1–14

Silverman J, Lazar B, Erez J (2007) Community metabolism of a coral reef exposed to naturally varying dissolved inorganic nutrient loads. Biogeochemistry 84:67–82

Silverstein RN, Correa AMS, Baker AC (2012) Specificity is rarely absolute in coral–algal symbiosis: Implications for coral response to climate change. Proc R Soc B Biol Sci 279:2609–2618

Silverstein RN, Cunning R, Baker AC (2015) Change in algal symbiont communities after bleaching, not prior heat exposure, increases heat tolerance of reef corals. Glob Chang Biol 21:236–249

Sinclair BJ, Williams CM, Terblanche JS (2012) Variation in Thermal Performance among Insect Populations. Physiol Biochem Zool 85:594–606

Stimson, John and Kinzie III RA (1991) The temporal pattern and rate of release of zooxanthellae from the reef coral *Pocillopora damicornis* (Linnaeus) under nitrogen-enrichment and control conditions m. J Exp Mar Bio Ecol 153:63–74

Szmant AM (2002) Nutrient Enrichment on Coral Reefs: Is It a Major Cause of Coral Reef Decline? Estuaries 25:743–766

Szmant AM, Forrester A (1996) Water column and sediment nitrogen and phosphorus distribution patterns in the Florida Keys, USA. Coral Reefs 15:21–41

Tanaka Y, Inoue M, Nakamura T, Suzuki A, Sakai K (2014) Loss of zooxanthellae in a coral under high seawater temperature and nutrient enrichment. J Exp Mar Bio Ecol 457:220–225

Tanaka Y, Suzuki A, Sakai K (2018) The stoichiometry of coral-dinoflagellate symbiosis: Carbon and nitrogen cycles are balanced in the recycling and double translocation system. ISME J 12:860–868

Veal CJ, Carmi M, Fine M, Hoegh-Guldberg O (2010) Increasing the accuracy of surface area estimation using single wax dipping of coral fragments. Coral Reefs 29:893–897

Vega Thurber RL, Burkepile DE, Fuchs C, Shantz AA, Mcminds R, Zaneveld JR (2014) Chronic nutrient enrichment increases prevalence and severity of coral disease and bleaching. Glob Chang Biol 20:544–554

Wall CB, Ricci CA, Foulds GE, Mydlarz LD, Gates RD, Putnam HM (2018) The effects of environmental history and thermal stress on coral physiology and immunity. Mar Biol 165:56

Wang L, Shantz AA, Payet JP, Sharpton TJ, Foster A, Burkepile DE, Thurber RV (2018) Corals and their microbiomes are differentially affected by exposure to elevated nutrients and a natural thermal anomaly. Front Mar Sci 5:1–16

Weis VM (2010) The susceptibility and resilience of corals to thermal stress: Adaptation, acclimatization or both?: NEWS and VIEWS. Mol Ecol 19:1515–1517

Wiedenmann J, D'Angelo C, Smith EG, Hunt AN, Legiret FE, Postle AD, Achterberg EP (2013) Nutrient enrichment can increase the susceptibility of reef corals to bleaching. Nat Clim Chang 3:160–164

Wilkinson C (2008) Status of coral reefs of the world: 2008. Global Coral Reef Monitoring Network and Reef and Rainforest Research Centre, Townsville, Australia.

Wolanski E, Delesalle B (1995a) Upwelling by internal waves, Tahiti, French Polynesia. Cont Shelf Res 15:357–368

Wolanski E, Delesalle B (1995b) Wind-driven upwelling in Opunohu Bay, Moorea, French Polynesia. Estuar Coast Shelf Sci 40:57–66

Wooldridge SA (2013) Breakdown of the coral-algae symbiosis: Towards formalising a linkage between warm-water bleaching thresholds and the growth rate of the intracellular zooxanthellae. Biogeosciences 10:1647–1658

Worm B, Sommer U (2000) Rapid direct and indirect effects of a single nutrient pulse in a seaweed-epiphyte-grazer system. Mar Ecol Prog Ser 202:283–288

Zaneveld JR, Burkepile DE, Shantz AA, Pritchard CE, McMinds R, Payet JP, Welsh R, Correa AMS, Lemoine NP, Rosales S, Fuchs C, Maynard JA, Thurber RV (2016) Overfishing and nutrient pollution interact with temperature to disrupt coral reefs down to microbial scales. Nat Commun 7:1–12